Inorg. Chem. **2008**, *47*, 11825−11838

Unusual Structural Types in Nickel Cluster Chemistry from the Use of Pyridyl Oximes: Ni_5, $Ni_{12}Na_2$, and Ni_{14} Clusters

Theocharis C. Stamatatos,[†] Albert Escuer,[§] Khalil A. Abboud,[†] Catherine P. Raptopoulou,[⊥] Spyros P. Perlepes,*[,‡] and George Christou*[,†]

Department of Chemistry, University of Florida, Gainesville, Florida, 32611-7200, Departament de Quimica Inorganica, Universitat de Barcelona, Diagonal 647, 08028 Barcelona, Spain, Institute of Materials Science, NCSR "Demokritos", 153 10 Aghia Paraskevi Attikis, Greece, and Department of Chemistry, University of Patras, Patras 26504, Greece

Received August 14, 2008

Syntheses, crystal structures, and magnetochemical characterization are reported for the three new nickel(II) clusters $[Ni_{14}(OH)_4(N_3)_8(pao)_{14}(paoH)_2(H_2O)_2](ClO_4)_2$ (**1**), $[Ni_{12}Na_2(OH)_4(N_3)_8(pao)_{12}(H_2O)_{10}](OH)_2$ (**2**), and $[Ni_5(ppko)_5(H_2O)_7](NO_3)_5$ (**3**) (paoH = pyridine-2-carbaldehyde oxime, ppkoH = di-2-pyridyl ketone oxime). The reaction of $Ni(ClO_4)_2 \cdot 6H_2O$ with paoH and $NBu^n_4N_3$ in H_2O/MeCN in the presence of NEt_3, gave **1** in 65% yield. Complex **2** was obtained in 60% yield from the reaction of $NiCl_2 \cdot 6H_2O$ with paoH and NaN_3 in H_2O/MeCN in the presence of NaOH. The reaction of $Ni(NO_3)_2 \cdot 6H_2O$ with ppkoH in EtOH in the presence of LiOH afforded complex **3** in 75% yield. The complexes all contain novel core topologies. The core of **1** comprises a central Ni_4 rhombus between two Ni_5. Complex **1** is the largest metal/oxime cluster discovered to date, as well as the first Ni^{II}_{14} coordination complex and the largest Ni^{II}/N_3^- cluster. Complex **2** has a $Ni_{12}Na_2$ topology that is very similar to that of **1**, but with two central Ni^{II} atoms of **1** replaced with Na^I atoms. The core of **3** consists of four Ni^{II} atoms forming a highly distorted tetrahedron, with the fifth Ni^{II} atom lying almost on one of the edges. Variable-temperature, solid-state dc susceptibility and magnetization studies were carried out on complexes **1**−**3**, and these were complemented with ac susceptibility data for **1** and **2**. Fitting of the obtained $M/(N\mu_B)$ vs H/T data by matrix diagonalization and including axial zero-field splitting (D) gave ground-state spin (S) and D values of $S = 6$, $D = -0.12(3)$ cm^{-1} for **1** and $S = 3$, $D = -0.20(5)$ cm^{-1} for each of the two essentially noninteracting $S = 3$ Ni_6 subunits of **2**. The data for **3** indicate antiferromagnetic exchange interactions and an $S = 1$ ground state. A simple 2-J model was found to be adequate to describe the variable-temperature dc susceptibility data. The combined work demonstrates the ligating flexibility of pao^- and $ppko^-$, and their usefulness in the synthesis of polynuclear Ni_x clusters with or without the presence of ancillary ligands.

Introduction

The last 20 years have witnessed an explosive growth in interest in the polynuclear complexes (clusters) of 3d metals at intermediate oxidation states with primarily oxygen- or nitrogen-based ligation.[1] Reasons for this include the search for various nuclearity oxide-bridged metal clusters to model M_x sites in biomolecules, including understanding the growth of the core of the iron storage protein ferritin,[2] and synthesis of models for the Mn site of water oxidation within the photosynthetic apparatus of green plants and cyanobacteria.[3] In addition, high-nuclearity 3d metal clusters often display interesting and occasionally novel magnetic properties, including high ground-state spin values,[4] and single-molecule magnetism behavior.[5,6] The latter are molecules with both a large ground-state spin (S) and a significant easy-axis magnetic anisotropy, as reflected in a negative zero-field

* To whom correspondence should be addressed. E-mail: christou@chem.ufl.edu (G.C.), perlepes@patreas.upatras.gr (S.P.P.).
[†] University of Florida.
[§] University of Barcelona.
[⊥] NCSR "Demokritos".
[‡] University of Patras.

(1) (a) Winpenny, R. E. P. In *Comprehensive Coordination Chemistry II*; McCleverty, J. A., Meyer, T. J., Eds.; Elsevier: Amsterdam, 2004; Vol *7*, pp 125−175. (b) Stamatatos, Th. C.; Christou, G. *Philos. Trans. R. Soc. A* **2008**, *366*, 113.
(2) For a minireview, see: Theil, E. C.; Matzapetakis, M.; Liu, X. *J. Biol. Inorg. Chem.* **2006**, *11*, 803.

10.1021/ic801555e CCC: $40.75
Published on Web 11/12/2008

splitting parameter (D). Single-molecule magnets (SMMs) function as nanoscale magnetic particles at sufficiently low temperatures and represent a molecular, or "bottom-up", route to nanoscale magnetism[7] with potential applications in information storage and molecular spintronics[7a] and use as quantum bits (qbits) in quantum computation.[7b] Although Mn clusters have proven to be the most fruitful source of high-spin molecules and SMMs, complexes displaying SMM behavior are known for several other 3d metals,[8] including heterometallic 3d/4f complexes.[9,10]

The future health of the field of 3d metal clusters and the chances of discovering high-spin molecules or new SMMs will both benefit from the continuing development of new synthetic procedures for high-nuclearity species. There are now several empirically established approaches to a variety of clusters.[11] In Mn and Fe chemistry, for example, alcoholysis has proven to be a very useful method for obtaining both oxo- and hydroxo-containing complexes.[12] Another fertile approach is the use of alcohol or oxime ligands, since alkoxides[13] and oximates[14] are good bridging groups and thus foster formation of polynuclear products. 2-Pyridyl oximes[15] and 2,6-pyridyl dioximes[15,16] (Scheme 1) are popular ligands whose anions are versatile ligands for a variety of research objectives; the activation of 2-pyridyl oximes by 3d metal centers toward further reaction is also becoming a fruitful area of research.[17] Such ligands have been key "players" in several areas of single-molecule[18,19] and single-chain magnetism.[20] We recently reported,[19] for example, the use of methyl 2-pyridyl ketone oxime (mpkoH) to prepare $[Mn^{III}_3O(O_2CR')_3(mpko)_3]^+$ complexes that were the initial examples of triangular SMMs, by switching the exchange coupling from the usual antiferromagnetic to ferromagnetic.

Efforts to date by us[16b,19,21] and other groups[16a,22] with 2-pyridyl oximes and 2,6-pyridyl dioximes have mainly concentrated on Mn chemistry, but we have recently

Scheme 1

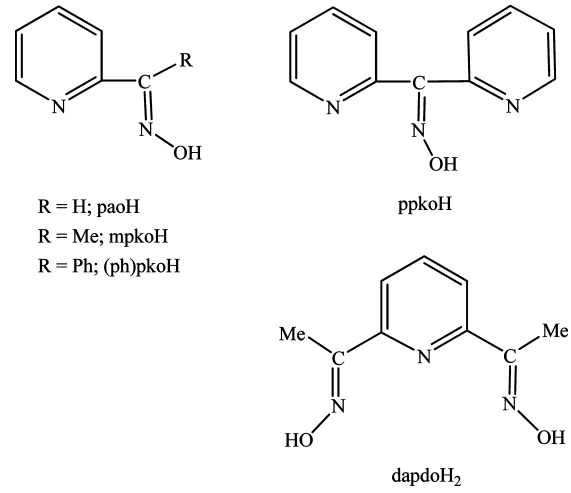

(3) For recent comprehensive reviews concerning this topic, see: (a) Mullins, C. J.; Pecoraro, V. L. *Coord. Chem. Rev.* **2008**, *252*, 416. (b) Barber, J.; Murray, J. W. *Coord. Chem. Rev.* **2008**, *252*, 433.

(4) (a) Ako, A. M.; Hewitt, I. J.; Mereacre, V.; Clérac, R.; Wernsdorfer, W.; Anson, C. E.; Powell, A. K. *Angew. Chem., Int. Ed.* **2006**, *45*, 4926. (b) Stamatatos, Th. C.; Abboud, K. A.; Wernsdorfer, W.; Christou, G. *Angew. Chem., Int. Ed.* **2007**, *46*, 884. (c) Low, D. M.; Rajaraman, G.; Helliwell, M.; Timco, G.; van Slageren, J.; Sessoli, R.; Ochsenbein, S. T.; Bircher, R.; Dobe, C.; Waldman, O.; Güdel, H.-U.; Adams, M. A.; Ruiz, E.; Alvarez, S.; McInnes, E. J. L. *Chem.—Eur. J.* **2006**, *12*, 1385. (d) Manoli, M.; Johnstone, R. D. L.; Parsons, S.; Murrie, M.; Affronte, M.; Evangelisti, M.; Brechin, E. K. *Angew. Chem., Int. Ed.* **2007**, *46*, 4456. (e) Stamatatos, Th. C.; Poole, K. M.; Abboud, K. A.; Wernsdorfer, W.; O'Brien, Th. A.; Christou, G. *Inorg. Chem.* **2008**, *47*, 5006.

(5) For reviews, see: (a) Bagai, R.; Christou, G. *Chem. Soc. Rev.*, in press. (b) Birchner, R.; Chaboussant, G.; Dobe, C.; Güdel, H.; Ochsenbein, S. T.; Sieber, A.; Waldman, O. *Adv. Funct. Mater.* **2006**, *16*, 209. (c) Gatteschi, D.; Sessoli, R. *Angew. Chem., Int. Ed.* **2003**, *42*, 268. (d) Long, J. R. In *Chemistry of Nanostructured Materials*; Yang, P., Ed.; World Scientific Publishing: Hong Kong, 2003; p 291. (e) Christou, G.; Gatteschi, D.; Hendrickson, D. N.; Sessoli, R. *MRS Bull.* **2000**, *25*, 66.

(6) (a) Chakov, N. E.; Lee, S.-C.; Harter, A. G.; Kuhns, P. L.; Reyes, A. P.; Hill, S. O.; Dalal, N. S.; Wernsdorfer, W.; Abboud, K. A.; Christou, G. *J. Am. Chem. Soc.* **2006**, *128*, 6975. (b) Milios, C. J.; Vinslava, A.; Wernsdorfer, W.; Moggach, S.; Parsons, S.; Perlepes, S. P.; Christou, G.; Brechin, E. K. *J. Am. Chem. Soc.* **2007**, *129*, 2754.

(7) (a) Bogani, L.; Wernsdorfer, W. *Nat. Mater.* **2008**, *7*, 179. (b) Leuenberger, M. N.; Loss, D. *Nature* **2001**, *410*, 789.

(8) For a comprehensive review, see: Aromi, G.; Brechin, E. K. *Struct. Bonding (Berlin)* **2006**, *122*, 1.

(9) (a) Murugesu, M.; Mishra, A.; Wernsdorfer, W.; Abboud, K. A.; Christou, G. *Polyhedron* **2006**, *25*, 613. (b) Ferbinteanu, M.; Kajiwara, T.; Choi, K.-W.; Nojiri, H.; Nakamoto, A.; Kojima, N.; Cimpoesu, F.; Fujimura, Y.; Takaishi, S.; Yamashita, M. *J. Am. Chem. Soc.* **2006**, *128*, 9008.

(10) (a) Mishra, A.; Wernsdorfer, W.; Abboud, K. A.; Christou, G. *J. Am. Chem. Soc.* **2004**, *126*, 15648. (b) Mishra, A.; Wernsdorfer, W.; Parsons, S.; Christou, G.; Brechin, E. K. *Chem. Commun.* **2005**, 2086. (c) Mereacre, V. M.; Ako, A. M.; Clerac, R.; Wernsdorfer, W.; Filoti, G.; Bartolome, J.; Anson, C. E.; Powell, A. K. *J. Am. Chem. Soc.* **2007**, *129*, 9248.

(11) (a) Christou, G. *Polyhedron* **2005**, *24*, 2065. (b) Winpenny, R. E. P. *J. Chem. Soc., Dalton Trans.* **2002**, 1.

(12) Tasiopoulos, A. J.; Vinslava, A.; Wernsdorfer, W.; Abboud, K. A.; Christou, G. *Angew. Chem., Int. Ed.* **2004**, *43*, 2117. (b) Canada-Vilalta, C.; O'Brien, T. A.; Pink, M.; Davidson, E. R.; Christou, G. *Inorg. Chem.* **2003**, *42*, 7819.

(13) For reviews describing the use of such chelates in transition metal cluster chemistry, see: (a) Tasiopoulos, A. J.; Perlepes, S. P. *Dalton Trans.* **2008**, 5537. (b) Brechin, E. K. *Chem. Commun.* **2005**, 5141. (c) Papaefstathiou, G. S.; Perlepes, S. P. *Comments Inorg. Chem.* **2002**, *23*, 249.

(14) For a review describing the use of the oximate group in transition metal chemistry, see: Chaudhuri, P. *Coord. Chem. Rev.* **2003**, *243*, 143.

(15) For a comprehensive review, see: Milios, C. J.; Stamatatos, Th. C.; Perlepes, S. P. *Polyhedron* **2005**, *25*, 134.

(16) (a) Khanra, S.; Weyhermüller, Th.; Chaudhuri, P. *Dalton Trans.* **2007**, 4675. (b) Stamatatos, Th. C.; Luisi, B. S.; Moulton, B.; Christou, G. *Inorg. Chem.* **2008**, *47*, 1134. (c) Khanra, S.; Weyhermüller, Th.; Chaudhuri, P. *Dalton Trans.* **2007**, 4675.

(17) (a) Milios, C. J.; Kyritsis, P.; Raptopoulou, C. P.; Terzis, A.; Vicente, R.; Escuer, A.; Perlepes, S. P. *Dalton Trans.* **2005**, 501. (b) Milios, C. J.; Kefalloniti, E.; Raptopoulou, C. P.; Terzis, A.; Escuer, A.; Vicente, R.; Perlepes, S. P. *Polyhedron* **2004**, *23*, 83. (c) Kumagai, H.; Endo, M.; Kondo, M.; Kawata, S.; Kitagawa, S. *Coord. Chem. Rev.* **2003**, *237*, 197.

(18) (a) Mori, F.; Ishida, T.; Nogami, T. *Polyhedron* **2005**, *24*, 2588. (b) Mori, F.; Nyui, T.; Ishida, T.; Nogami, T.; Choi, K.-Y.; Nojiri, H. *J. Am. Chem. Soc.* **2006**, *128*, 1440.

(19) (a) Stamatatos, Th. C.; Foguet-Albiol, D.; Stoumpos, C. C.; Raptopoulou, C. P.; Terzis, A.; Wernsdorfer, W.; Perlepes, S. P.; Christou, G. *J. Am. Chem. Soc.* **2005**, *127*, 15380. (b) Stamatatos, Th. C.; Foguet-Albiol, D.; Stoumpos, C. C.; Raptopoulou, C. P.; Terzis, A.; Wernsdorfer, W.; Perlepes, S. P.; Christou, G. *Polyhedron* **2007**, *26*, 2165. (c) Stamatatos, Th. C.; Foguet-Albiol, D.; Lee, S.-C.; Stoumpos, C. C.; Raptopoulou, C. P.; Terzis, A.; Wernsdorfer, W.; Hill, S. O.; Perlepes, S. P.; Christou, G. *J. Am. Chem. Soc.* **2007**, *129*, 9484. (d) Lee, S.-C.; Stamatatos, Th. C.; Foguet-Albiol, D.; Hill, S.; Perlepes, S. P.; Christou, G. *Polyhedron* **2007**, *26*, 2255.

extended our work to Ni chemistry. SMMs containing Ni^{II}[8,23] are far less common than Mn ones, despite the fact that mononuclear Ni complexes have $|D| > 10$ cm^{-1}.[24] In the present work, we have used 2-pyridinealdoxime (paoH; pyridine-2-carbaldehyde oxime) and di-2-pyridyl ketone oxime (ppkoH; dipyridin-2-yl-methanone oxime) for the synthesis of some interesting new Ni^{II} clusters. The use of paoH in Ni chemistry had previously given $[Ni_3(pao)_5(paoH)]^{+}$[25] and $[Ni_9(OH)_4(pao)_{10}(H_2O)_8]^{4+}$,[26] and we have now discovered routes to two significantly higher nuclearity species, $Ni_{12}Na_2$ and Ni_{14}. Similarly, ppkoH has been previously used in carboxylate,[27] as well as mixed-ligand,[28] Ni chemistry by both Kessissoglou and co-workers and our group; for example, the former have reported the remarkable cluster $[Ni_4(ppko)_6(MeOH)_2]^{2+}$.[29] We suspected that there might be a number of other high-nuclearity Ni^{II}_x/ppko$^-$ species available, and we have now discovered a Ni_5 member of this family. The syntheses, structures, and magnetochemical characterization of these Ni_{14}, $Ni_{12}Na_2$, and Ni_5 complexes are described in this paper. A portion of this work has been previously communicated.[30]

Experimental Section

Syntheses. All manipulations were performed under aerobic conditions using reagents and solvents as received. $NBu^n_4N_3$ was prepared as described elsewhere.[31] **Warning***! Azide and perchlorate salts are potentially explosive; such compounds should be synthesized and used in small quantities and treated with utmost care at all times*.

$[Ni_{14}(OH)_4(N_3)_8(pao)_{14}(paoH)_2(H_2O)_2](ClO_4)_2$ (1). Method A. To a pale green solution of $Ni(ClO_4)_2\cdot 6H_2O$ (0.37 g, 1.01 mmol) in H_2O (20 mL) was added solid paoH (0.12 g, 0.98 mmol). The resulting olive-green solution was stirred for 15 min, during which time an aqueous solution of NaOH (1 M) was added in small portions until the pH adjusted to 8.0. The homogeneous solution was treated with a solution of NaN_3 (0.13 g, 2.00 mmol) in H_2O (5 mL) to give an olive-green precipitate. The stirring was maintained for an additional 10 min. The solid product was isolated by filtration, washed with cold H_2O (1 × 3 mL), and dried in air for 24 h. Dissolution of the solid in MeCN (25 mL) and layering with a solvent mixture comprising Et_2O/Me_2CO (50 mL, 1:1 v/v) gave olive-green crystals of $\mathbf{1}\cdot 4Me_2CO\cdot 2Et_2O\cdot 6H_2O$ after 10 days. The crystals were collected by filtration, washed with cold Me_2CO (1 × 3 mL) and Et_2O (2 × 5 mL), and dried under vacuum. Yield 15% (based on the ligand). The dried solid was determined by analysis to be solvent-free **1**. Anal. Calcd for $C_{96}H_{90}Ni_{14}N_{56}O_{30}Cl_2$: C, 33.90; H, 2.67; N, 23.07; Cl, 2.08%. Found: C, 33.76; H, 2.75; N, 22.97; Cl, 1.99%. IR (KBr, cm^{-1}): 3440sh, 3397mb, 2950w, 2062vs, 1620sh, 1603s, 1531s, 1473m, 1425w, 1344m, 1293m, 1222m, 1089sb, 1040s, 990m, 889m, 773s, 683s, 637m, 622m, 570m, 535w, 450m.

Method B. To a pale green solution of $Ni(ClO_4)_2\cdot 6H_2O$ (0.37 g, 1.01 mmol) in H_2O (10 mL) was added solid paoH (0.12 g, 0.98 mmol). The resulting olive-green solution was stirred for 15 min, during which time NEt_3 (0.14 mL, 1.00 mmol) was added in small portions. The homogeneous solution was treated with $NBu^n_4N_3$ (0.48 g, 2.00 mmol) in MeCN (15 mL) to give a clear olive-green solution. This was stirred for 5 min more and filtered, and the filtrate was layered with a solvent mixture comprising Et_2O/Me_2CO (50 mL, 1:3 v/v). After 5 days, olive-green crystals of $\mathbf{1}\cdot 4Me_2CO\cdot 2Et_2O\cdot 6H_2O$ were collected by filtration, washed with cold Me_2CO (2 × 2 mL) and Et_2O (2 × 5 mL), and dried under vacuum. Yield 65% (based on the ligand). The identity of the product was confirmed by elemental analyses (C, H, N, Cl) and IR spectroscopic comparison with authentic material from method A. Anal. Calcd for $C_{96}H_{90}Ni_{14}N_{56}O_{30}Cl_2$: C, 33.90; H, 2.67; N, 23.07; Cl, 2.08%. Found: C, 34.11; H, 2.37; N, 23.39; Cl, 1.90%.

$[Ni_{12}Na_2(OH)_4(N_3)_8(pao)_{12}(H_2O)_{10}](OH)_2$ (2). To a pale green solution of $NiCl_2\cdot 6H_2O$ (0.25 g, 1.00 mmol) in H_2O (20 mL) was

(20) (a) Clérac, R.; Miyasaka, H.; Yamashita, M.; Coulon, C. *J. Am. Chem. Soc.* **2002**, *124*, 12837. (b) Miyasaka, H.; Clérac, R.; Mizushima, K.; Sugiura, K.; Yamashita, M.; Wernsdorfer, W.; Coulon, C. *Inorg. Chem.* **2003**, *42*, 8203.

(21) (a) Milios, C. J.; Stamatatos, Th. C.; Kyritsis, P.; Terzis, A.; Raptopoulou, C. P.; Vicente, R.; Escuer, A.; Perlepes, S. P. *Eur. J. Inorg. Chem.* **2004**, 2885. (b) Stoumpos, C. C.; Stamatatos, Th. C.; Psycharis, V.; Raptopoulou, C. P.; Christou, G.; Perlepes, S. P. *Polyhedron*, in press. (c) Stoumpos, C. C.; Stamatatos, Th. C.; Sartzi, H.; Roubeau, O.; Tasiopoulos, A. J.; Nastopoulos, V.; Teat, S. J.; Perlepes, S. P.; Christou, G. *Dalton Trans.* **2008**, accepted for publication.

(22) (a) Zaleski, C. M.; Weng, T.-C.; Dendrinou-Samara, C.; Alexiou, M.; Kanakaraki, P.; Hsieh, W.-Y.; Kampf, J.; Penner-Hahn, J. E.; Pecoraro, V. L.; Kessissoglou, D. P. *Inorg. Chem.* **2008**, *47*, 6127. (b) Roubeau, O.; Lecren, L.; Li, Y.-G.; Le Goff, X. F.; Clérac, R. *Inorg. Chem. Commun.* **2005**, *8*, 314. (c) Dendrinou-Samara, C.; Zaleski, C. M.; Evagorou, A.; Kampf, J. W.; Pecoraro, V. L.; Kessissoglou, D. P. *Chem. Commun.* **2003**, 2668. (d) Alexiou, M.; Dendrinou-Samara, C.; Karagianni, A.; Biswas, S.; Zaleski, C. M.; Kampf, J.; Yoder, D.; Penner-Hahn, J. E.; Pecoraro, V. L.; Kessissoglou, D. P. *Inorg. Chem.* **2003**, *42*, 2185. (e) Alexiou, M.; Zaleski, C. M.; Dendrinou-Samara, C.; Kampf, J.; Kessissoglou, D. P.; Pecoraro, V. L. *Z. Anorg. Allg. Chem.* **2003**, *629*, 2348. (f) Afrati, T.; Dendrinou-Samara, C.; Raptopoulou, C. P.; Terzis, A.; Tangoulis, V.; Kessissoglou, D. P. *Angew. Chem., Int. Ed.* **2002**, *41*, 2148.

(23) (a) Andres, H.; Basler, R.; Blake, A. J.; Cadiou, C.; Chaboussant, G.; Grant, C. M.; Güdel, H.-U.; Murrie, M.; Parsons, S.; Paulsen, C.; Semadini, F.; Villar, V.; Wernsdorfer, W.; Winpenny, R. E. P. *Chem.—Eur. J.* **2002**, *8*, 4867. (b) Ochsenbein, S. T.; Murrie, M.; Rusanov, E.; Stoeckli-Evans, H.; Sekime, C.; Güdel, H.-U. *Inorg. Chem.* **2002**, *41*, 5133. (c) Yang, E.-C.; Wernsdorfer, W.; Hill, S.; Edwards, R. S.; Nakano, M.; Maccagano, S.; Zakharov, L. N.; Rheingold, A. L.; Christou, G.; Hendrickson, D. N. *Polyhedron* **2003**, *22*, 1727. (d) Moragues-Cànovas, M.; Helliwell, M.; Ricard, L.; Rivière, E.; Wernsdorfer, W.; Brechin, E.; Mallah, T. *Eur. J. Inorg. Chem.* **2004**, 2219. (e) Bell, A.; Aromi, G.; Teat, S. J.; Wernsdorfer, W.; Winpenny, R. E. P. *Chem. Commun.* **2005**, 2808. (f) Aromi, G.; Parsons, S.; Wernsdorfer, W.; Brechin, E. K.; McInnes, E. J. L. *Chem. Commun.* **2005**, 5038. (g) Yang, E.-C.; Wernsdorfer, W.; Zakharov, L. N.; Karaki, Y.; Yamaguchi, A.; Isidro, R. M.; Lu, G.; Wilson, S. A.; Rheingold, A. L.; Ishimoto, H.; Hendrickson, D. N. *Inorg. Chem.* **2006**, *45*, 529.

(24) (a) Rogez, G.; Rebilly, J.-N.; Barra, A.-L.; Sorace, L.; Blondin, G.; Kirchner, N.; Duran, M.; van Slageren, J.; Parsons, S.; Ricard, L.; Marvilliers, A.; Mallah, T. *Angew. Chem., Int. Ed.* **2005**, *44*, 1876. (b) Krzystek, J.; Park, J. H.; Meisel, M. W.; Hitchman, M. A.; Stratemeier, H.; Brunel, L. C.; Telser, J. *Inorg. Chem.* **2002**, *41*, 4478.

(25) Weyhermüller, Th.; Wagner, R.; Khanra, S.; Chaudhuri, P. *Dalton Trans.* **2005**, 2539.

(26) (a) Khanra, S.; Weyhermüller, Th.; Rentschler, E.; Chaudhuri, P. *Inorg. Chem.* **2005**, *44*, 8176. (b) Stamatatos, Th. C.; Diamantopoulou, E.; Tasiopoulos, A.; Psycharis, V.; Vicente, R.; Raptopoulou, C. P.; Nastopoulos, V.; Escuer, A.; Perlepes, S. P. *Inorg. Chim. Acta* **2006**, *359*, 4149.

(27) Stamatatos, Th. C.; Diamantopoulou, E.; Raptopoulou, C. P.; Psycharis, V.; Escuer, A.; Perlepes, S. P. *Inorg. Chem.* **2007**, *46*, 2350.

(28) (a) Psomas, G.; Stemmler, A. J.; Dendrinou-Samara, C.; Bodwin, J. J.; Schneider, M.; Alexiou, M.; Kampf, J. W.; Kessissoglou, D. P.; Pecoraro, V. L. *Inorg. Chem.* **2001**, *40*, 1562. (b) Alexiou, M.; Tsivikas, I.; Dendrinou-Samara, C.; Pantazaki, A. A.; Trikalitis, P.; Lalioti, N.; Kyriakidis, D. A.; Kessissoglou, D. P. *J. Inorg. Biochem.* **2003**, *93*, 256.

(29) Alexiou, M.; Dendrinou-Samara, C.; Raptopoulou, C. P.; Terzis, A.; Tangoulis, V.; Kessissoglou, D. P. *Eur. J. Inorg. Chem.* **2004**, 3822.

(30) Stamatatos, Th. C.; Abboud, K. A.; Perlepes, S. P.; Christou, G. *Dalton Trans.* **2007**, 3861.

(31) Firouzabadi, H.; Iranpoor, N.; Garzan, A.; Shaterian, H. R.; Ebrahimzadeh, F. *Eur. J. Org. Chem.* **2005**, 416.

added solid paoH (0.12 g, 0.98 mmol). The solid soon dissolved, and the resulting olive-green solution was stirred for 5 min, during which time an aqueous solution of NaOH (1 M) was added in small portions until the pH was adjusted to 8.0. The homogeneous solution was treated with a solution of NaN_3 (0.13 g, 2.00 mmol) in H_2O (5 mL) to give an olive precipitate. The stirring was maintained for 15 min more. The solid product was isolated by filtration, washed with cold H_2O (1 × 3 mL), and dried in air for 24 h. Dissolution of the solid in MeCN (25 mL) and layering with Et_2O (50 mL) gave dark orange crystals of **2**·6Et_2O after 3 days. The crystals were collected by filtration, washed with cold MeCN (2 × 2 mL) and Et_2O (2 × 5 mL), and dried in air. Yield 60% (based on the ligand). The dried material is hygroscopic and was determined by analysis to be **2**·2H_2O. Anal. Calcd for $C_{72}H_{90}Ni_{12}Na_2N_{48}O_{30}$: C, 30.25; H, 3.18; N, 23.52. Found: C, 30.22; H, 3.26; N, 23.37%. IR (KBr, cm^{-1}): 3442s, 3392s, ∼3200mb, 2962w, 2059vs, 1625m, 1602s, 1526s, 1473s, 1433m, 1342m, 1293m, 1251w, 1224m, 1120s, 1085m, 891mb, 776m, 765sh, 683m, 642m, 558w, 532w, 443m.

$[Ni_5(ppko)_5(H_2O)_7](NO_3)_5$ (3). To a green solution of $Ni(NO_3)_2$·6H_2O (0.29 g, 0.96 mmol) in EtOH (20 mL) was added a colorless solution of ppkoH (0.20 g, 1.00 mmol) and LiOH·H_2O (0.04 g, 1.00 mmol) in the same solvent (10 mL). The resulting dark red solution was stirred for 20 min and filtered, and the filtrate was left undisturbed at room temperature to concentrate slowly by evaporation. After 2 days, dark red crystals of **3**·1.5EtOH·2H_2O were collected by filtration, washed with cold EtOH (2 × 2 mL), and dried in air. Yield 75% (based on the ligand). The dried material is slightly hygroscopic and was determined by analysis to be **3**·2H_2O. Anal. Calcd for $C_{55}H_{58}Ni_5N_{20}O_{29}$: C, 37.60; H, 3.33; N, 15.95. Found: C, 37.49; H, 3.42; N, 15.79%. IR (KBr, cm^{-1}): 3368mb, 1600m, 1554s, 1469m, 1413m, 1384vs, 1214m, 1162m, 1125m, 1088m, 1059m, 1022m, 977m, 825m, 792m, 754m, 705m, 631m, 449m.

X-ray Crystallography. Data for complexes **1**·4Me_2CO·2Et_2O·6H_2O and **2**·6Et_2O were collected on a Siemens SMART PLATFORM equipped with a CCD area detector and a graphite monochromator utilizing Mo Kα radiation (λ = 0.71073 Å). Suitable crystals were attached to glass fibers using silicone grease and transferred to a goniostat where they were cooled to 173 K for data collection. An initial search for reciprocal space revealed a triclinic cell for both complexes; the choice of space group $P\bar{1}$ was confirmed by the subsequent solution and refinement of the structures. Cell parameters were refined using up to 8192 reflections. A full sphere of data (1850 frames) was collected using the ω-scan method (0.3° frame width). The first 50 frames were remeasured at the end of data collection to monitor instrument and crystal stability (maximum correction on I was <1%). Absorption corrections by integration were applied based on measured indexed crystal faces. The structures were solved by direct methods in *SHELXTL6*[32] and refined on F^2 using full-matrix least-squares. The non-H atoms were treated anisotropically, whereas the H atoms were placed in calculated, ideal positions and refined as riding on their respective C atoms.

For **1**·4Me_2CO·2Et_2O·6H_2O, all ClO_4^- counteranions and lattice solvent molecules were disordered and could not be modeled properly; thus, the program *SQUEEZE*,[33] a part of the PLATON package of crystallographic software, was used to calculate the solvent disorder area and remove its contribution to the overall intensity data. Due to the rather low quality of the data, the ClO_4^- anions could not be quantified and refined, and thus the charge balance for the $\{Ni_{14}\}^{2+}$ cations could not be ascertained crystallographically. However, elemental analysis data (C, H, N, Cl) verify the presence of two ClO_4^- anions per cation. The refinement of the $\{Ni_{14}\}^{2+}$ cations provides the molecular connectivity, but bond distances and angles are probably not very reliable. There were a few restraints applied to fix bond distances of certain atoms that did not refine well. A total of 793 parameters were included in the structure refinement using 4447 reflections with $I > 2\sigma(I)$ to yield R_1 and wR_2 of 8.28% and 18.13%, respectively.

For **2**·6Et_2O, the solvent molecules were disordered and could not be modeled properly, and thus the program *SQUEEZE* was used to calculate the solvent disorder area and remove its contribution to the overall intensity data. A total of 739 parameters were included in the structure refinement using 8180 reflections with $I > 2\sigma(I)$ to yield R_1 and wR_2 of 3.52% and 6.15%, respectively.

A crystal of **3**·1.5EtOH·2H_2O was mounted in a capillary filled with drops of mother liquor. Data were collected using a Crystal Logic Dual Goniometer diffractometer with a graphite monochromator utilizing Mo Kα radiation. Unit cell dimensions were determined and refined by using the angular settings of 25 automatically centered reflections in the range 11° < 2θ < 23°. Intensity data were recorded using a $\theta-2\theta$ scan to a max 2θ value of 47.0°. Three standard reflections monitored every 97 reflections showed less than 3% variation and no decay. Lorentz polarization corrections were applied using Crystal Logic Software. The structure was solved by direct methods using *SHELXS-86*[34a] and refined by full-matrix least-squares on F^2 with *SHELXL-97*.[34b] The H atoms on H_2O molecules were located by difference maps and refined isotropically; the rest were introduced at calculated positions as riding on their parent respective atoms. All non-H atoms were refined anisotropically. One of the NO_3^- ions was found to be disordered and refined in two orientations with occupancies adding up to 100%. One of the solvate EtOH molecules was refined isotropically with occupation factor fixed at 0.5.

Unit cell parameters and structure solution and refinement data are listed in Table 1. CCDC reference numbers are 640087, 640088, and 697348.

Physical Studies. Elemental analyses (C, H, N, Cl) were performed by the in-house facilities of the Chemistry Department, University of Florida. IR spectra (4000−450 cm^{-1}) were recorded using Nicolet Nexus 670 FT-IR and Perkin-Elmer 16 PC spectrometers with samples as KBr pellets. Variable-temperature dc and ac magnetic susceptibility data for **1** and **2** were collected at the University of Florida using a Quantum Design MPMS-XL SQUID magnetometer equipped with a 7 T magnet; the samples were embedded in eicosane to prevent torquing. Variable-temperature magnetic studies for **3** were performed using a Quantum Design SQUID magnetometer at the Magnetochemistry Service of the University of Barcelona. Diamagnetic corrections were applied to the observed paramagnetic susceptibilities using Pascal's constants.

Results and Discussion

Syntheses and IR Spectra. The two previously established structural types in Ni^{II}/paoH cluster chemistry are characterized by antiferromagnetic exchange interactions. Thus, the ground-state spin of both $[Ni_3(pao)_5(paoH)]^{+}$[25] and $[Ni_9(OH)_4(pao)_{10}(H_2O)_8]^{4+}$[26] is S = 1, with the exchange

(32) *SHELXTL6*; Bruker-AXS, Madison, WI, 2000.

(33) van der Sluis, P.; Spek, A. L. *Acta Crystallogr., Sect. A* **1990**, *46*, 194.

(34) (a) Sheldrick, G. M. *SHELXS-86, Program for Crystal Structure Solution*; University of Göttingen, Germany, 1997. (b) Sheldrick, G. M. *SHELXL-97, Program for the Refinement of Crystal Structures from Diffraction Data*; University of Göttingen, Germany, 1997.

Table 1. Crystallographic Data for Complexes $1\cdot 4Me_2CO\cdot 2Et_2O\cdot 6H_2O$, $2\cdot 6Et_2O$, and $3\cdot 1.5EtOH\cdot 2H_2O$

	1	2	3
formula[a]	$C_{116}H_{146}Ni_{14}N_{56}O_{42}Cl_2$	$C_{96}H_{146}Ni_{12}Na_2N_{48}O_{34}$	$C_{58}H_{67}Ni_5N_{20}O_{30.5}$
mol wt, g mol^{-1}[a]	3889.72	3267.11	1825.89
crystal system	triclinic	triclinic	triclinic
space group	$P\bar{1}$	$P\bar{1}$	$P\bar{1}$
a, Å	17.143(6)	13.768(1)	17.680(9)
b, Å	20.214(7)	16.273(1)	14.989(9)
c, Å	25.715(9)	17.522(1)	15.584(8)
α, deg	83.38(1)	102.33(1)	98.27(2)
β, deg	82.21(1)	108.53(1)	96.17(2)
γ, deg	65.90(1)	107.78(1)	106.22(2)
V, Å^3	8041(5)	3328.3(5)	3877(4)
Z	2	1	2
T, K	173(2)	173(2)	298(2)
λ, Å[b]	0.71073	0.71073	0.71073
ρ_{calcd}, g cm^{-3}	1.607	1.629	1.552
μ, mm^{-1}	1.722	1.752	1.286
measured/unique	36302/22335	22866/14940	11828/11353
R_{int}	0.1731	0.0411	0.0232
observed[c]	4447	8180	8682
R_1[d,e]	0.0828	0.0352	0.0564
wR_2[e,f]	0.1813	0.0615	0.1498
GOF on F^2	0.603	0.761	1.075
$(\Delta\rho)_{max,min}$, e Å^{-3}	1.070, −0.656	0.789, −0.551	1.410, −0.844

[a] Including solvate molecules. [b] Mo Kα radiation. [c] $I > 2\sigma(I)$. [d] $R_1 = \sum(||F_o| - |F_c||)/\sum|F_o|$. [e] For observed $[I > 2\sigma(I)]$ reflections. [f] $wR_2 = [\sum[w(F_o^2 - F_c^2)^2]/\sum[w(F_o^2)^2]]^{1/2}$.

interactions being propagated by bridging OH^- or oximate groups. Our approach was to employ a second bridging ligand in the Ni^{II}/paoH reaction system that typically gives ferromagnetic interactions and that can thus increase the chances of a larger ground-state S value. The azide (N_3^-) ion bridging in the 1,1-fashion (end-on) is a strong ferromagnetic mediator for a wide range of M−N−M angles, and it thus represents a well recognized route to high-spin species and SMMs,[35] although its use in combination with pyridyl oximes is still in its infancy.[22a,36] We thus decided to explore Ni^{II} reactions with azide and the tridentate (*N*,*N*′,*O*) anionic ligand pao^-.

The 1:1 reaction between $Ni(ClO_4)_2\cdot 6H_2O$ and paoH in H_2O gave an olive-green solution. When the pH was adjusted to 8.0 using aqueous NaOH (1 M) to help the deprotonation of paoH ($pK_a = 10.01$) and the solution was treated with 2 equiv of aqueous NaN_3, an olive-green solid was precipitated. Crystallization from $MeCN/Et_2O/Me_2CO$ gave olive-green crystals of $1\cdot 4Me_2CO\cdot 2Et_2O\cdot 6H_2O$ in a low (∼15%) overall yield. The formation of **1** is summarized in eq 1.

$$14Ni^{2+} + 16paoH + 18OH^- + 8N_3^- \rightarrow [Ni_{14}(OH)_4(N_3)_8(pao)_{14}(paoH)_2(H_2O)_2]^{2+} + 12H_2O \quad (1)$$

To increase the yield of **1**, the colored filtrates were allowed to slowly evaporate at room temperature. This gave a mixture of small olive-green plates and microcrystalline dark orange prisms, in a visual ratio of ∼1:4. Some olive-green plates were manually separated and were spectroscopically (IR) identical to **1**. The IR spectrum of the dark orange material indicated the presence of N_3^- groups and the absence of ClO_4^- ions; the latter was confirmed by a zero Cl analysis. We were unable to improve the crystallinity sufficiently to crystallographically identify this orange material, but this was subsequently accomplished by the alternative route below.

Since ClO_4^- ions were essential for yielding the cationic complex **1**, the $Ni(ClO_4)_2\cdot 6H_2O$ reagent was replaced with $NiCl_2\cdot 6H_2O$ in the hope that this would divert the reaction away from **1**. Indeed, the reaction of $NiCl_2\cdot 6H_2O$ with paoH and NaN_3 in an 1:1:2 molar ratio in H_2O, employing aqueous NaOH to raise the pH to 8.0, gave a dull green precipitate, which was crystallized from an $MeCN/Et_2O$ layering to give well-formed dark orange crystals in high yield (∼60%) of what was crystallographically identified as $2\cdot 6Et_2O$. We were pleased to see that the IR spectrum of **2** was identical to that of the dark orange crystals from the filtrate in the procedure for **1**. The formation of **2** can be summarized in eq 2.

$$12Ni^{2+} + 12paoH + 16OH^- + 8N_3^- \rightarrow [Ni_{12}Na_2(OH)_4(N_3)_8(pao)_{12}(H_2O)_{10}]^{2+} + 2H_2O \quad (2)$$

With the identities of **1** and **2** established, a convenient high-yield synthesis of **1** was easily developed by avoiding the presence of Na^+ in the reaction. The reaction (method B) of $Ni(ClO_4)_2\cdot 6H_2O$ with paoH, NEt_3, and $NBu^n_4N_3$ in a 1:1:1:2 ratio in $H_2O/MeCN$ gave an olive-green solution and the subsequent isolation of **1** in high yields (∼65%). This reaction also used NEt_3 in place of NaOH as the proton acceptor to facilitate the deprotonation of paoH groups and H_2O molecules as a source of the OH^- ions. The excess N_3^- used in the preparation of **1** (by method B) and **2** is beneficial to the yields; when stoichiometric amounts were used, the yields were lower than 30%. Various reactions with other Ni^{II} non-carboxylate sources, such as $NiSO_4$ or $NiBr_2$, gave noncrystalline materials that we were not able to further characterize.

(35) For a microreview, see: (a) Escuer, A.; Aromi, G. *Eur. J. Inorg. Chem.* **2006**, 4721. (b) Stamatatos, Th. C.; Abboud, K. A.; Wernsdorfer, W.; Christou, G. *Angew. Chem., Int. Ed.* **2008**, *47*, 6694. (c) Liu, T.-F.; Fu, D.; Gao, S.; Zhang, Y.-Z.; Sun, H.-L.; Su, G.; Liu, Y.-J. *J. Am. Chem. Soc.* **2003**, *125*, 13976. (d) Xu, H.-B.; Wang, B.-W.; Pan, F.; Wang, Z.-M.; Gao, S. *Angew. Chem., Int. Ed.* **2007**, *46*, 7388.

(36) Milios, C. J.; Piligkos, S.; Bell, A. R.; Laye, R. H.; Teat, S. J.; Vicente, R.; McInnes, E. J. L.; Escuer, A.; Perlepes, S. P.; Winpenny, R. E. P. *Inorg. Chem. Commun.* **2006**, *9*, 638.

As stated earlier, the only previously characterized Ni^{II}/ppko$^-$ cluster without additional carboxylates or other anionic ligands was $[Ni_4(ppko)_6(MeOH)_2](ClO_4)(OH)$.[29] In our own work with ppkoH, we were investigating the use of Ni nitrate as reagent and a Ni/ppkoH ratio of 1:1, and we found that our reaction systems gave a distinctly different product. Thus, the 1:1:1 reaction between $Ni(NO_3)_2 \cdot 6H_2O$, ppkoH, and LiOH in EtOH gave $[Ni_5(ppko)_5(H_2O)_7](NO_3)_5$ (**3**); the formation of **3** is summarized in eq 3. The same product was also obtained from MeOH.

$$5Ni^{2+} + 5ppkoH + 5OH^- + 2H_2O \rightarrow [Ni_5(ppko)_5(H_2O)_7]^{5+} \quad (3)$$

With the identity of **3** established, we also tried several other $Ni(NO_3)_2 \cdot 6H_2O$/ppkoH/OH^- ratios, particularly with an excess of the Ni salt, to see whether higher nuclearity products might be obtained, but in all cases, complex **3** was the product isolated, in varying yields. The LiOH was essential for a good yield, but too much rapidly gave insoluble precipitates. Using NaOH in place of LiOH led again to complex **3** but in appreciably lower yields (~5−10%).

The presence of neutral oxime groups in **1**, OH^- ions in **1** and **2**, and aqua ligands/H_2O solvate molecules is manifested by one to three bands at 3450−3200 cm^{-1} assigned to ν(OH); their broadness and relatively low frequency are both indicative of hydrogen bonding. The in-plane deformation of the 2-pyridyl ring of free paoH at 627 cm^{-1} shifts upward on coordination within **1** (637 cm^{-1}) and **2** (642 cm^{-1}).[37] Several bands appear in the 1625−1400 cm^{-1} region for **1**−**3**; contributions from the $\nu(C{=}N)_{oximate/oxime}$ and δ(OH) modes (>1580 cm^{-1}) are expected in this region, but overlap with the stretching vibrations of the aromatic ring(s) renders assignments and discussion of the coordination shifts difficult. The medium band at 985 cm^{-1} for free paoH is assigned to the $\nu(NO)_{oxime}$ mode,[38] which increases to 1040 and 1085 cm^{-1} in **1** and **2**, respectively. This shift to higher frequencies has been discussed and is in accord with the fact that upon deprotonation and oximate-*O* coordination, there is a higher contribution of N=O to the electronic structure of the oximate group; consequently the ν(NO) vibration shifts to a higher frequency relative to that for paoH.[26b,38] The medium intensity band at 990 cm^{-1} in the spectrum of **1** is thus consistent with the presence of neutral paoH groups containing uncoordinated oxygen atoms. The $\nu(NO)_{oximate}$ vibration appears at 1125 cm^{-1} in **3**. The IR spectra of **1** and **2** exhibit an intense band at ~2060 cm^{-1}, which is assigned to the asymmetric stretching mode, ν_{as}(NNN), of the end-on azide group.[39] The spectrum of **1** exhibits a strong band at 1089 cm^{-1} and a medium band at 622 cm^{-1}, due to the $\nu_3(F_2)[\nu_d(ClO)]$ and $\nu_4(F_2)[\delta_d(OClO)]$ modes, respectively, of the uncoordinated T_d ClO_4^- ions.[40] The very strong band at 1384 cm^{-1} in **3**, attributed to the $\nu_3(E')$ mode of the D_{3h} NO_3^- group, indicates the presence of ionic nitrates.[40]

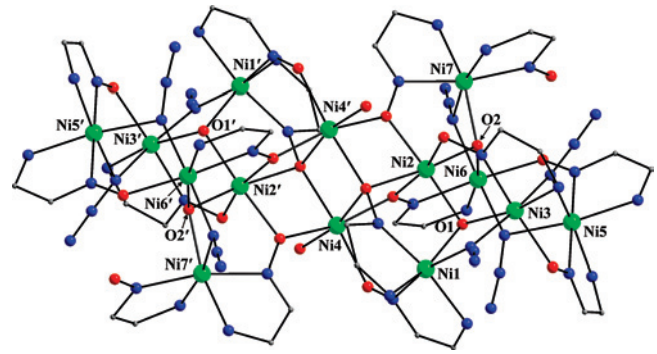

Figure 1. Partially labeled plot of the Ni_{14} cation of **1**. To avoid congestion, most C atoms of the pao$^-$ and paoH ligands have been omitted. Color scheme: Ni, green; O, red; N, blue; C, gray. Primed and unprimed atoms are related by the crystallographic inversion center.

Description of Structures. Complex **1**·$4Me_2CO \cdot 2Et_2O \cdot 6H_2O$ crystallizes in the triclinic space group $P\bar{1}$, with the asymmetric unit consisting of two Ni_{14} half-cations lying on crystallographic inversion centers, two ClO_4^- anions, four Me_2CO, two Et_2O, and six H_2O solvate molecules; the latter four will not be further discussed. The partially labeled structure of the $[Ni_{14}(OH)_4(N_3)_8(pao)_{14}(paoH)_2(H_2O)_2]^{2+}$ cation is shown in Figure 1 and two views of its core are illustrated in Figures 2 (top) and 3. Selected interatomic distances and angles are listed in Table 2.

The cation consists of 14 Ni^{II} atoms held together by four μ_3-OH^- ions (O1, O2, O1′, O2′), eight end-on bridging μ-N_3^- ions, and eight $\eta^1{:}\eta^1{:}\eta^1{:}\mu$ (O4, O5, O6, O7 and their symmetry equivalents), four $\eta^1{:}\eta^1{:}\eta^2{:}\mu_3$ (O8, O9, and their symmetry equivalents), and two $\eta^1{:}\eta^1{:}\eta^3{:}\mu_4$ (O3 and O3′) pao$^-$ ligands; where multiple η values are given; they are indicating the hapticity of each donor atom rather than the whole polydentate pao$^-$ or paoH group, that is, the number of metal atoms to which a donor atom is attached. Peripheral ligation is provided by two bidentate chelating neutral paoH groups on Ni7 and Ni7′, and two terminal aqua ligands on central Ni4 and Ni4′. The core (Figure 2, top) can be described as a central $\{Ni_4(\mu_3\text{-}OR')_2(\mu\text{-}OR')_4\}^{2+}$ defective double cubane ($R'O^- = pao^-$) linked to two $\{Ni_5(\mu\text{-}N_3)_4(\mu\text{-}OH)_2\}^{4+}$ subunits via the two OH^- groups of each of the latter, which become μ_3 (Figure S1 in Supporting Information). Although Ni_4 complexes containing the defective double-cubane $[Ni_4(\mu_3\text{-}OR')_2(\mu\text{-}OR')_4]^{2+}$ core have been reported,[41] the $\{Ni_5(\mu\text{-}N_3)_4(\mu\text{-}OH)_2\}^{4+}$ subunit present in **1** has not been observed either in a discrete Ni_5 cluster or as a recognizable subfragment of higher nuclearity Ni clusters. If we consider all the bridging oximate groups as part of the core, then the latter is $[Ni_{14}(\mu_3\text{-}OH)_4(\mu\text{-}N_3)_8(\mu_4\text{-}ONR'')_2(\mu_3\text{-}ONR'')_4(\mu\text{-}ONR'')_8]^{2+}$ ($R''NO^- = pao^-$) (Figure 3).

Ni1 and Ni7 are bound to an ON_5 set of donor atoms, Ni3 and Ni6 to an O_2N_4 set, Ni2 and Ni4 to an O_6 set, and

(37) Lever, A. B. P.; Mantovani, E. *Inorg. Chem.* **1971**, *10*, 817.
(38) (a) Chaudhuri, P.; Winter, M.; Flörke, U.; Houpt, H.-J. *Inorg. Chim. Acta* **1995**, *232*, 125. (b) Papatriantafyllopoulou, C.; Raptopoulou, C. P.; Terzis, A.; Manessi-Zoupa, E.; Perlepes, S. P. *Z. Naturforsch.* **2006**, *61b*, 37.
(39) Stamatatos, Th. C.; Papaefstathiou, G. S.; MacGillivray, L. R.; Escuer, A.; Vicente, R.; Ruiz, E.; Perlepes, S. P. *Inorg. Chem.* **2007**, *46*, 8843.
(40) Nakamoto, K. *Infrared and Raman Spectra of Inorganic and Coordination Compounds*, 4th ed.; Wiley: New York, 1986.
(41) For example, see: Efthymiou, C. G.; Raptopoulou, C. P.; Terzis, A.; Boèa, R.; Korabic, M.; Mrozinski, J.; Perlepes, S. P.; Bakalbassis, E. G. *Eur. J. Inorg. Chem.* **2006**, 2236.

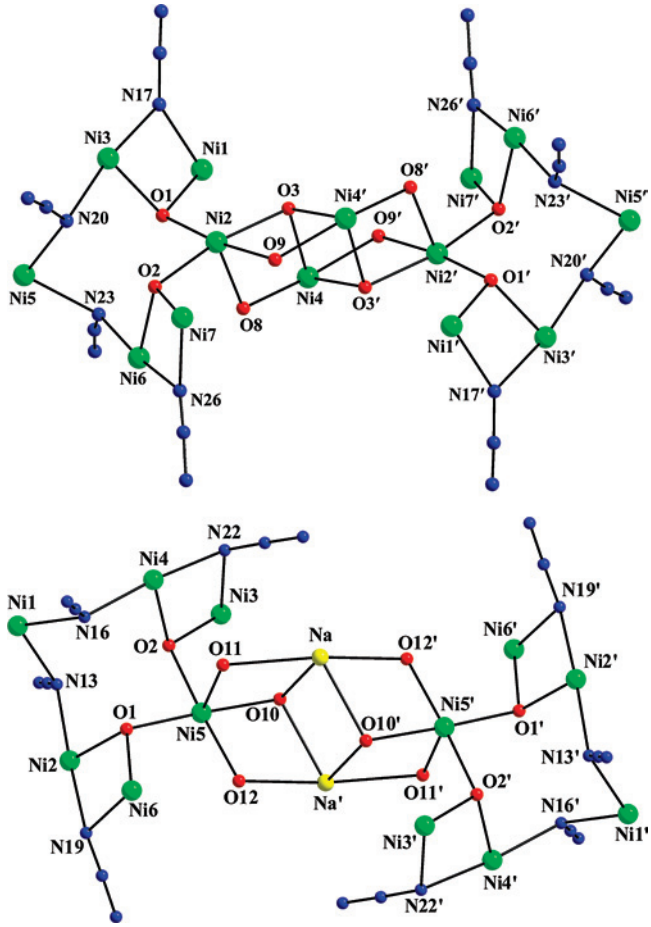

Figure 2. The $[Ni_{14}(\mu_3\text{-}OH)_4(\mu\text{-}N_3)_8(\mu_3\text{-}OR')_2(\mu\text{-}OR')_4]^{10+}$ core of **1** (top) and the $[Ni_{12}Na_2(\mu_3\text{-}OH)_4(\mu\text{-}N_3)_8(\mu_3\text{-}OR')_2(\mu\text{-}OR')_4]^{8+}$ core of **2** (bottom). Color scheme: Ni, green; Na, yellow; O, red; N, blue; C, gray. O1, O1′, O2, and O2′ are the hydroxide O atoms, while O3−O12 and their symmetry equivalents belong to the oximate groups of the pao$^-$ ligands.

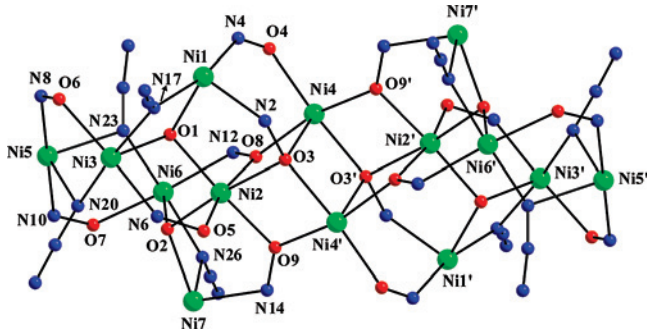

Figure 3. A more detailed view of the core of **1** emphasizing its $[Ni_{14}(\mu_3\text{-}OH)_4(\mu\text{-}N_3)_8(\mu_4\text{-}ONR'')_2(\mu_3\text{-}ONR'')_4(\mu\text{-}ONR'')_8]^{2+}$ description; color scheme as in Figure 1. O1, O1′, O2, and O2′ are the hydroxide O atoms, while O3−O9 and their symmetry equivalents belong to the oximate groups of the pao$^-$ ligands.

Ni5 is unique in forming a NiN_6 chromophore. Thus all the Ni^{II} atoms are six-coordinate with distorted octahedral geometries, the main distortion arising from the relatively small bite angle of the chelating parts of the pao$^-$/paoH groups. There is a range of Ni···Ni separations, depending on the number and the nature of the bridges between the metal atoms: Ni^{II} atoms separated by two monatomic bridges (N_3^- and OH^-, or two oximate oxygens) have the shortest separations [3.173(1)−3.317(2) Å]. The μ-N_3^- atoms N23 and N26 bridge the Ni^{II} atoms asymmetrically; thus, the Ni6−N23 [2.051(12) Å] and Ni6−N26 [2.045(13) Å] bonds are shorter than the Ni5−N23 [2.191(12) Å] and Ni7−N26 [2.162(12) Å] ones. The Ni−N_{azido}−Ni angles are in the 94.7(6)°−111.1(6)° range. The larger angles [108.5(6)°, 111.1(6)°] correspond to the pairs (Ni3/Ni5 and Ni5/Ni6) in which the Ni^{II} atoms are singly bridged by one N_3^- group, whereas the smaller ones [94.7(6)°, 98.2(5)°] correspond to the metal ions (Ni1/Ni3 and Ni6/Ni7) bridged by one N_3^- group and one OH^- ion. The coordination geometry at the hydroxo oxygen atoms (O1, O2) is pyramidal, while the Ni−$O_{oximate}$−Ni angles are in the 97.4(4)°−106.0(5)° range.

Table 2. Selected Interatomic Distances (Å) and Angles (deg) for Complex **1**·4Me_2CO·2Et_2O·6H_2O[a]

Ni1···Ni2	3.379(8)	Ni3−N20	2.169(14)
Ni1···Ni3	3.173(10)	Ni4−O3	2.174(9)
Ni2···Ni3	3.390(10)	Ni4−O3′	2.085(9)
Ni2···Ni4	3.220(9)	Ni4−O4	2.033(5)
Ni2···Ni4′	3.255(10)	Ni4−O8	2.068(11)
Ni2···Ni7	3.366(10)	Ni4−O9′	2.087(10)
Ni4···Ni4′	3.317(10)	Ni4−O11	2.098(9)
Ni5···Ni5′	14.749(8)	Ni5−N7	2.023(12)
Ni1−O1	2.065(10)	Ni5−N8	2.054(14)
Ni1−N1	2.080(8)	Ni5−N9	2.088(13)
Ni1−N2	1.975(12)	Ni5−N10	2.057(13)
Ni1−N3	2.069(10)	Ni5−N20	2.139(13)
Ni1−N4	2.254(18)	Ni5−N23	2.191(12)
Ni1−N17	2.116(14)	Ni6−O2	2.063(8)
Ni2−O1	2.025(9)	Ni6−O7	2.080(10)
Ni2−O2	2.061(10)	Ni6−N11	2.077(12)
Ni2−O3	2.113(10)	Ni6−N12	2.096(13)
Ni2−O5	2.014(9)	Ni6−N23	2.051(12)
Ni2−O8	2.029(9)	Ni6−N26	2.045(13)
Ni2−O9	1.989(9)	Ni7−O2	2.040(9)
Ni3−O1	2.053(9)	Ni7−N13	1.999(12)
Ni3−O6	2.055(10)	Ni7−N14	2.095(12)
Ni3−N5	2.144(12)	Ni7−N15	2.070(12)
Ni3−N6	2.014(11)	Ni7−N16	2.080(15)
Ni3−N17	2.196(16)	Ni7−N26	2.162(12)
Ni1−O1−Ni2	111.4(4)	Ni4−O3−Ni4′	102.3(4)
Ni1−O1−Ni3	100.8(4)	Ni2−O8−Ni4	103.6(4)
Ni2−O1−Ni3	112.5(4)	Ni2−O9−Ni4′	106.0(5)
Ni2−O2−Ni6	110.3(4)	Ni1−N17−Ni3	94.7(6)
Ni2−O2−Ni7	110.4(4)	Ni3−N20−Ni5	108.5(6)
Ni6−O2−Ni7	101.6(4)	Ni5−N23−Ni6	111.1(6)
Ni2−O3−Ni4	97.4(4)	Ni6−N26−Ni7	98.2(5)
Ni2−O3−Ni4′	101.7(4)		

[a] Symmetry code: (′) = $-x$, $-y$, $-z$.

Complex **1** is the largest metal/oxime cluster discovered to date, as well as the first Ni_{14} coordination complex and the largest Ni^{II}/N_3^- cluster. While the number of polynuclear complexes of 3d metals at intermediate oxidation states continues to grow rapidly, some nuclearities remain rare. Tetradecanuclear 3d metal complexes are particularly rare, and complex **1** thus becomes a new member of the small family of M_{14} complexes, which currently comprises $V^{III}_8V^{IV}_6$,[42] Cr^{III}_{14},[42] $Mn^{II}_{12}Mn^{III}_2$,[43a] $Mn^{II}_{10}Mn^{III}_4$,[43b] $Mn^{II}_6Mn^{III}_8$,[43c] $Mn^{II}_4Mn^{III}_{10}$,[43d] $Fe^{II}_2Fe^{III}_{12}$,[44a] Fe^{III}_{14},[42,44b,c] $Co^{II}_8Co^{III}_6$,[45] Co^{III}_{14},[46] $Cu^{I}_2Cu^{II}_{12}$,[47] and Cu^{II}_{14}[48] clusters. Complex **1** also joins only a handful of previous Ni^{II} coordination clusters, that is, non-organometallic, with a nuclearity equal to or larger than 14. We have listed them

(42) Shaw, R.; Laye, R. H.; Jones, L. F.; Low, D. M.; Talbot-Eeckelaers, C.; Wei, Q.; Milios, C. J.; Teat, S.; Helliwell, M.; Raftery, J.; Evangelisti, M.; Affronte, M.; Collison, D.; Brechin, E. K.; McInnes, E. J. L. *Inorg. Chem.* **2007**, *46*, 4968.

Table 3. Formulas and Ground State *S* Values for Polynuclear Ni^{II} Coordination Complexes with Nuclearities ≥ 14

complex[a]	*S*	ref.
$[Ni_{24}(O_2CMe)_{42}(mdaH)_6(EtOH)_6]$	6	49
$[Ni_{24}(OH)_8(O_2CMe)_{24}(mpo)_{16}(mpoH)_{16}]$	24	50
$[Ni_{21}(OH)_{10}(cit)_{12}(H_2O)_{10}]^{16-}$	3	23b, 51
$[Ni_{21}Ag(OH)_{10}(O_2CBu^t)_{20}(fpo)_{13}(BuCO_2H)_4(MeCN)_3(H_2O)]$	3	52
$[Ni_{16}Na_2(O_2CMe)_{20}(HCO_2)_2(mdaH)_{12}]$	*b*	53
$[Ni_{14}(OH)_4(N_3)_8(pao)_{14}(paoH)_2(H_2O)_2]^{2+}$	6	*c*

[a] Counterions and solvate molecules have been omitted. Heterometallic clusters with more than 14 Ni^{II} atoms are also included in this table. Abbreviations: cit = the tetraanion of citric acid; fpo = the monoanion of 3-trifluoromethyl-3-pyrazolin-5-one; mdaH = the monoanion of N-methyldiethanolamine; mpo = the monoanion of 3-methyl-3-pyrazolin-5-one; pao = the monoanion of pyridine-2-carbaldehyde oxime; mpoH and paoH are the neutral ligands 3-methyl-3-pyrazolin-5-one and pyridine-2-carbaldehyde oxime, respectively. [b] An accurate determination was not possible. [c] This work.

in Table 3 for a convenient comparison of their formulas and ground-state spin (*S*) values. Examination of Table 3 shows that the cation of **1** is one of the largest Ni^{II} clusters prepared to date, with only five known examples at higher nuclearity. Complex **1** is also remarkable because it contains the paoH/pao$^-$ ligands in four different coordination modes (Scheme 2), one of which is the unprecedented $\eta^1{:}\eta^1{:}\eta^3{:}\mu_4$ mode for pao$^-$.[15]

Complex **2**·6Et_2O crystallizes in the triclinic space group $P\bar{1}$. The asymmetric unit consists of half of a $[Ni_{12}Na_2(OH)_4(N_3)_8(pao)_{12}(H_2O)_{10}]^{2+}$ cation lying on an inversion center, a OH^- anion strongly hydrogen-bonded to the cation, and three Et_2O solvate molecules; the latter two will not be further discussed. It should be mentioned that OH^- counterions are with precedent in Ni^{II} cluster chemistry.[26b] The partially labeled structure of the cation is shown in Figure 4 and its core is illustrated in Figure 2 (bottom). Selected interatomic distances and angles are listed in Table 4.

The 12 Ni^{II} and two Na^I atoms in the centrosymmetric cation are held together by four μ_3-OH^- groups (O1, O2, O1′, O2′), eight end-on bridging (μ) N_3^- ions, and six $\eta^1{:}\eta^1{:}\mu$ (O7, O8, O9, and their symmetry equivalents), four $\eta^1{:}\eta^1{:}\eta^2{:}\mu_3$ (O11, O12, and their symmetry equivalents), and two $\eta^1{:}\eta^1{:}\eta^3{:}\mu_4$ (O10 and O10′) pao$^-$ groups (Scheme 2). The core is $[Ni_{12}Na_2(\mu_3\text{-}OH)_4(\mu\text{-}N_3)_8(\mu_3\text{-}OR')_2(\mu\text{-}OR')_4]^{8+}$ ($R'O^- =$ pao$^-$). If we consider all the bridging oximate groups as part of the core, then it is $[Ni_{12}Na_2(\mu_3\text{-}OH)_4(\mu\text{-}N_3)_8(\mu_4\text{-}ONR'')_2(\mu_3\text{-}ONR'')_4(\mu\text{-}ONR'')_6]^{2+}$ ($R''NO^-$ = pao$^-$); see Figure S2, Supporting Information. The cation of **2** is thus structurally very similar to that of **1**, the only differences being (i) the replacement of two $\eta^1{:}\eta^1{:}\eta^1{:}\mu$ pao$^-$ and the two η^2 paoH ligands of **1** by eight terminal H_2O ligands in **2**, (ii) the replacement of the two central octahedral Ni4 and Ni4′ atoms of **1** (Figures 1 and 2 (top)) with two square pyramidal Na^+ ions in **2** [$\tau = 0.21$;[54] Na···Na = 3.457(1) Å], and (iii) a twist of the central $\{Na_2O_2\}$ rhomb in **2** versus the $\{Ni_2O_2\}$ rhomb in **1**. The chromophores in **2** are $Ni1N_6$, $Ni(2,4)O_2N_4$, $Ni(3,6)O_3N_3$, and $Ni5O_6$; the Na^I atom is NaO_5, with one of the μ_3-oximate oxygens (O10′) at the apical position. Complex **2** is the second largest Ni^{II}/N_3^- cluster after **1**, joining only a handful of structurally characterized Ni^{II}_{12} coordination clusters.[55] It also joins a small family of Ni^{II}/Na^I clusters.[23e,53,56]

Overall, **1** and **2** are members of a relatively small family of mononuclear[57] and dinuclear/polynuclear (both homo-[25,26,58a] and heterometallic[25,58]) Ni^{II} complexes with neutral paoH or anionic pao$^-$ ligands.

Complex **3**·1.5EtOH·2H_2O crystallizes in the triclinic space group $P\bar{1}$. The asymmetric unit consists of a $[Ni_5(ppko)_5(H_2O)_7]^{5+}$ cation, five NO_3^- anions, and EtOH and H_2O solvate molecules. The partially labeled cation and its core are shown in Figures 5 and 6, respectively; selected interatomic distances and angles are listed in Table 5. The five Ni^{II} atoms are held together by four $\eta^1{:}\eta^1{:}\eta^2{:}\eta^1{:}\mu_3$ (O1, O11, O21, and O31) and one $\eta^1{:}\eta^1{:}\eta^1{:}\mu$ (O41) ppko$^-$ groups, see Scheme 2. In addition, there are two *trans* terminal H_2O ligands each on Ni1, Ni3, and Ni4, and a unique H_2O ligand on Ni2. The core is $[Ni_5(\mu_3\text{-}ONR'')_4(\mu\text{-}ONR'')]^{5+}$ ($R''NO^-$

(43) (a) Aromi, G.; Bell, A.; Teat, S. J.; Whittacker, A. G.; Winpenny, R. E. P. *Chem. Commun.* **2002**, 1896. (b) Milios, C. J.; Kefalloniti, E.; Raptopoulou, C. P.; Terzis, A.; Vicente, R.; Lalioti, N.; Escuer, A.; Perlepes, S. P. *Chem. Commun.* **2003**, 819. (c) Stamatatos, Th. C.; Abboud, K. A.; Christou, G. Unpublished results. (d) Xiao, F.-P.; Jin, L.-F. *Inorg. Chem. Commun.* **2008**, *11*, 719.

(44) (a) Bennett, M. V.; Holm, R. H. *Angew. Chem., Int. Ed.* **2006**, *45*, 5613. (b) Low, D. M.; Jones, L. F.; Bell, A.; Brechin, E. K.; Mallah, T.; Rivière, E.; Teat, S. J.; McInnes, E. J. L. *Angew. Chem., Int. Ed.* **2003**, *42*, 3781. (c) Grapperhaus, C. A.; O'Toole, M. G.; Mashuta, M. S. *Inorg. Chem. Commun.* **2006**, *9*, 1204.

(45) Aromi, G.; Batsanov, A. S.; Christian, P.; Helliwell, M.; Parkin, A.; Parsons, S.; Smith, A. A.; Timco, G. A.; Winpenny, R. E. P. *Chem.—Eur. J.* **2003**, *9*, 5142.

(46) Denisova, T. O.; Golubnichaya, M. A.; Nevedov, S. E. *Russ. Chem. Bull., Int. Ed.* **2003**, *52*, 2760.

(47) Mukherjee, A.; Nethaji, M.; Chakravarty, A. R. *Angew. Chem., Int. Ed.* **2004**, *43*, 87.

(48) (a) Tandon, S. S.; Bunge, S. D.; Thompson, L. K. *Chem. Commun.* **2007**, 798. (b) Willet, R. D. *J. Coord. Chem.* **1988**, *19*, 253.

(49) Foguet-Albiol, D.; Abboud, K. A.; Christou, G. *Chem. Commun.* **2005**, 4282.

(50) Dearden, A. L.; Parsons, S.; Winpenny, R. E. P. *Angew. Chem., Int. Ed.* **2001**, *40*, 152.

(51) Murrie, M.; Stoeckli-Evans, H.; Güdel, H.-U. *Angew. Chem., Int. Ed.* **2001**, *40*, 1957.

(52) Aromi, G.; Bell, A.; Teat, S. J.; Winpenny, R. E. P. *Chem. Commun.* **2005**, 2927.

(53) Biswas, B.; Khanra, S.; Weyhermüller, T.; Chaudhuri, P. *Chem. Commun.* **2007**, 1059.

(54) Addison, A. W.; Rao, T. N.; Reedijk, J.; Rijn, J.; Verschoor, G. C. *J. Chem. Soc., Dalton Trans.* **1984**, 1349.

(55) (a) Benelli, C.; Blake, A. J.; Brechin, E. K.; Coles, S. J.; Graham, A.; Harris, S. G.; Meier, S.; Parkin, A.; Parsons, S.; Seddon, A. M.; Winpenny, R. E. P. *Chem.—Eur. J.* **2000**, *6*, 883. (b) Bai, Y.; Dang, D.-B.; Duan, C.-Y.; Song, Y.; Meng, Q.-J. *Inorg. Chem.* **2005**, *44*, 5972. (c) Cooper, G. J. T.; Newton, G. N.; Kogerler, P.; Long, D.-L.; Engelhardt, L.; Luban, M.; Cronin, L. *Angew. Chem., Int. Ed.* **2005**, *44*, 5972.

(56) For example, see: Aromi, G.; Bell, A. R.; Helliwell, M.; Raftery, J.; Teat, S. J.; Timco, G. A.; Roubeau, O.; Winpenny, R. E. P. *Chem.—Eur. J.* **2003**, *9*, 3024.

(57) (a) Miyasaka, H.; Mizushima, K.; Sugiura, K.; Yamashita, M. *Synth. Met.* **2003**, *137*, 1245. (b) Orama, M.; Saarinen, H.; Korvenranta, J. *Acta Chem. Scand.* **1989**, *43*, 407. (c) Miyasaka, H.; Furukawa, S.; Yanagida, S.; Sugiura, K.; Yamashita, M. *Inorg. Chim. Acta* **2004**, *357*, 1619.

(58) (a) Chaudhuri, P.; Weyhermüller, Th.; Wagner, R.; Khanra, S.; Biswas, B.; Bothe, E.; Bill, E. *Inorg. Chem.* **2007**, *46*, 9003. (b) Ross, S.; Weyhermüller, Th.; Bill, E.; Bothe, E.; Flörke, H.-U.; Wieghardt, K.; Chaudhuri, P. *Eur. J. Inorg. Chem.* **2004**, 984. (c) Ross, S.; Weyhermüller, Th.; Bill, E.; Wieghardt, K.; Chaudhuri, P. *Inorg. Chem.* **2001**, *40*, 6656. (d) Miyasaka, H.; Nezu, T.; Iwahori, F.; Furukawa, S.; Sugimoto, K.; Clérac, R.; Sugiura, K.; Yamashita, M. *Inorg. Chem.* **2003**, *42*, 4501. (e) Miyasaka, H.; Nezu, T.; Sugimoto, K.; Sugiura, K.; Yamashita, M.; Clérac, R. *Inorg. Chem.* **2004**, *43*, 5486.

Scheme 2. The Various Coordination Modes for the paoH, pao$^-$ and ppko$^-$ Groups in **1**−**3**[a]

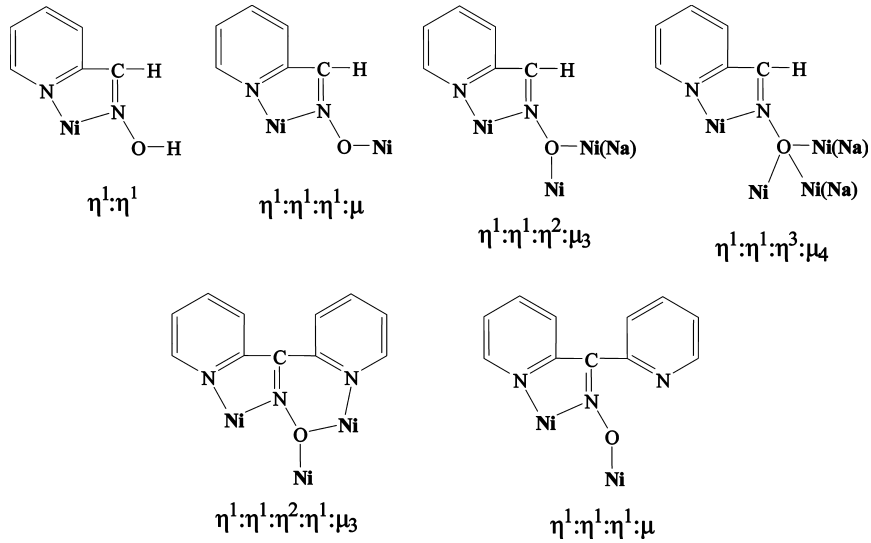

[a] Multiple η values refer to the number of metal atoms to which each ligand atom attaches.

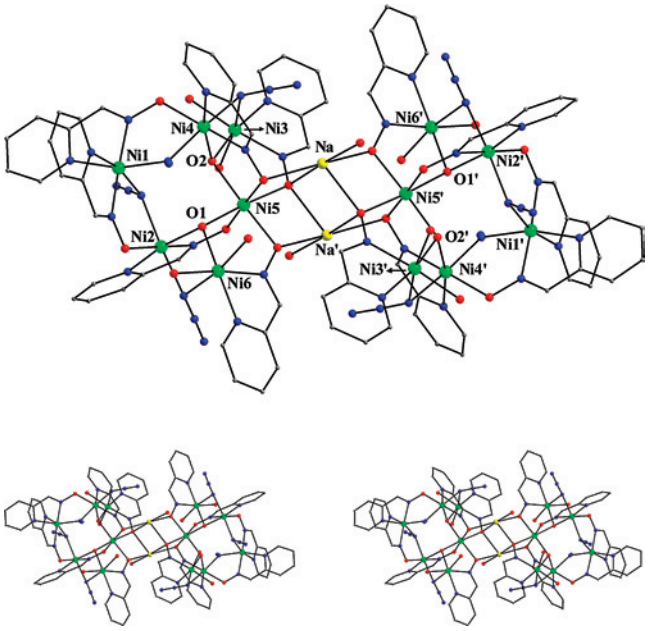

Figure 4. Partially labeled plot (top) and stereopair (bottom) of the $Ni_{12}Na_2$ cation of **2**, with H atoms omitted for clarity; color scheme as in Figure 2. Primed and unprimed atoms are related by the crystallographic inversion center.

= ppko$^-$). Atoms Ni1, Ni3, Ni4, and Ni5 form a highly distorted (flattened) tetrahedron (Figure 7), with the fifth metal atom (Ni2) lying not at the center of the tetrahedron but instead essentially at the midpoint of the Ni3−Ni4 edge; as a result, the Ni3−Ni2−Ni4 (173.2°) and Ni1−Ni2−Ni5 (140.6°) angles are much larger than the Ni1−Ni2−Ni3, Ni1−Ni2−Ni4, Ni3−Ni2−Ni5, and Ni4−Ni2−Ni5 angles (91.3°−94.8°). Each of the four μ_3-ppko$^-$ groups spans an edge of the Ni_4 tetrahedron and is ligated to the "central" metal (Ni2) through its doubly bridging oximate O atom. As a consequence, the Ni−Ni edges spanned by the μ_3-ppko$^-$ groups become shorter [4.714(3)−4.963(5) Å] than the two unspanned edges [Ni1−Ni5 = 6.058(8) Å, Ni3−Ni4 = 7.082(5) Å]. Due to the insertion of Ni2 between Ni3 and Ni4, the Ni3−Ni4 edge is the longest. The symmetry of the cation is destroyed due to the absence of two more μ_3-ppko$^-$ groups and the presence of a unique μ-ppko$^-$ group spanning the Ni2−Ni5 line. The Ni2−Ni(1,3,4,5) distances are in the 3.191(2)−3.728(3) Å range, shorter than the distances between the peripheral Ni^{II} atoms. The Ni_5 topology of **3** can also be described as a butterfly unit with three Ni^{II} atoms

Table 4. Selected Interatomic Distances (Å) and Angles (deg) for Complex **2**·6Et_2O[a]

Na···Na′	3.421(2)	Ni3−N22	2.149(3)
Na···Ni5	3.446(1)	Ni4−O2	2.009(2)
Na···Ni5′	3.457(1)	Ni4−O8	2.081(2)
Ni2···Ni6	3.129(2)	Ni4−N9	2.055(2)
Ni3···Ni4	3.159(5)	Ni4−N10	2.064(2)
Ni1···Ni4	3.494(7)	Ni4−N16	2.108(2)
Ni1···Ni2	3.493(3)	Ni4−N22	2.158(3)
Ni1···Ni1′	15.538(2)	Ni5−O1	2.043(2)
Ni1−N1	2.069(2)	Ni5−O2	2.049(2)
Ni1−N2	2.045(2)	Ni5−O9	2.123(2)
Ni1−N3	2.078(2)	Ni5−O10	2.039(2)
Ni1−N4	2.037(2)	Ni5−O11	2.142(2)
Ni1−N13	2.091(2)	Ni5−O12	2.035(2)
Ni1−N16	2.101(2)	Ni6−O1	2.023(2)
Ni2−O1	2.024(2)	Ni6−O3[b]	2.068(2)
Ni2−O7	2.089(2)	Ni6−O4[b]	2.095(2)
Ni2−N5	2.045(2)	Ni6−N11	2.077(3)
Ni2−N6	2.053(2)	Ni6−N12	2.033(2)
Ni2−N13	2.112(2)	Ni6−N19	2.141(2)
Ni2−N19	2.110(3)	Na−O10	2.452(2)
Ni3−O2	2.021(2)	Na−O10′	2.333(2)
Ni3−O5[b]	2.074(2)	Na−O11	2.394(2)
Ni3−O6[b]	2.094(2)	Na−O12′	2.339(2)
Ni3−N7	2.077(2)	Na−O13[b]	2.378(3)
Ni3−N8	2.030(2)		
Ni2−O1−Ni5	114.4(1)	Na′−O10−Ni5	104.3(1)
Ni2−O1−Ni6	101.3(1)	Na−O11−Ni5	98.8(1)
Ni5−O1−Ni6	111.7(1)	Na′−O12−Ni5	104.3(1)
Ni3−O2−Ni4	103.2(1)	Ni1−N13−Ni2	112.4(1)
Ni3−O2−Ni5	112.3(1)	Ni1−N16−Ni4	112.2(1)
Ni4−O2−Ni5	114.5(1)	Ni2−N19−Ni6	94.8(1)
Na−O10−Na′	91.3(1)	Ni3−N22−Ni4	94.4(1)
Na−O10−Ni5	99.8(1)		

[a] Symmetry code: (′) = −*x*, −*y*, −*z*. [b] These oxygen atoms belong to the terminal aqua ligands.

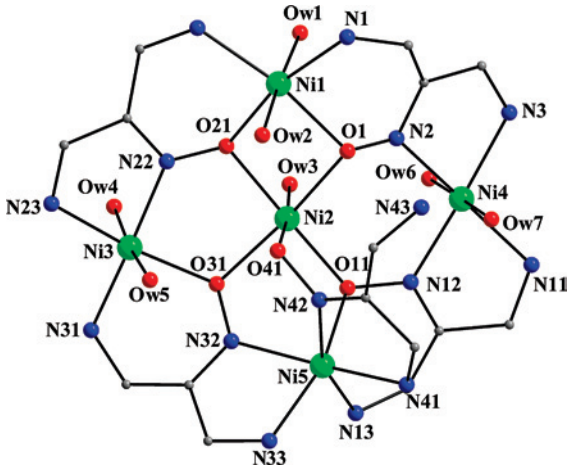

Figure 5. Partially labeled plot of the Ni_5 cation of **3**. To avoid congestion, most carbon atoms of the ppko$^-$ ligands, as well as all the H atoms, have been omitted; color scheme as in Figure 1. Atom N43 is the uncoordinated pyridyl nitrogen of the unique $\eta^1{:}\eta^1{:}\eta^1{:}\mu$ ppko$^-$ group.

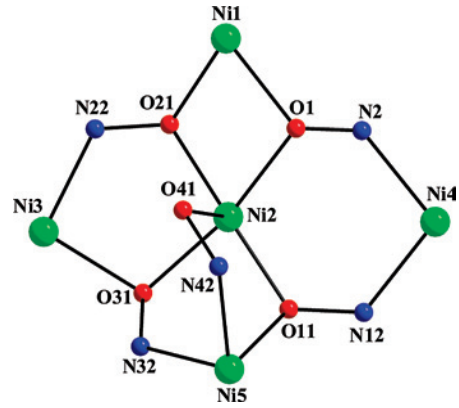

Figure 6. The $[Ni_5(\mu_3\text{-ONR}'')_4(\mu\text{-ONR}'')]^{5+}$ core of **3**; color scheme as in Figure 1.

at the "body" positions (Ni3, Ni2, Ni4) and two at the "wingtip" positions (Ni1, Ni5).

The five Ni^{II} atoms are six-coordinate with distorted octahedral geometries. The chromophores are all different, that is, $Ni1O_4N_2$, $Ni2O_6$, $Ni3O_3N_3$, $Ni4O_2N_4$, and $Ni5ON_5$. All bond lengths are typical for high-spin, six-coordinate Ni^{II} complexes.[25,26,59] There is an intramolecular H-bond between the OW7 H_2O ligand and the unbound pyridyl N43 atom, and much intermolecular H-bonding with the O atoms of H_2O ligands and the solvate molecules (EtOH, H_2O) as donors and the NO_3^- O atoms as acceptors. Complex **3** joins a rather large family of pentanuclear Ni^{II} clusters;[27,28a,59a,60] It is also a member of a small group of polynuclear Ni^{II} complexes of ppko$^-$,[27−29] a few of which also contain lanthanides[18a] or Mn^{III} atoms.[28a]

(59) (a) Tangoulis, V.; Raptopoulou, C. P.; Terzis, A.; Bakalbassis, E. G.; Diamantopoulou, E.; Perlepes, S. P. *Inorg. Chem.* **1998**, *37*, 3142. (b) Papatriantafyllopoulou, C.; Aromi, G.; Tasiopoulos, A. J.; Nastopoulos, V.; Raptopoulou, C. P.; Teat, S. J.; Escuer, A.; Perlepes, S. P. *Eur. J. Inorg. Chem.* **2007**, 2761.

(60) For example, see: (a) Velazquez, C. S.; Baumann, T. F.; Olmstead, M. M.; Hope, H.; Barrett, A. G. M.; Hoffman, B. M. *J. Am. Chem. Soc.* **1993**, *115*, 9997. (b) Shieh, S.-J.; Chou, C.-C.; Lee, G.-H.; Wang, C.-C.; Peng, S. M. *Angew. Chem., Int. Ed. Engl.* **1997**, *36*, 56.

Table 5. Selected Interatomic Distances (Å) and Angles (deg) for Complex **3**·1.5EtOH·2H_2O

Ni1···Ni2	3.191(2)	Ni2−O41	2.161(4)
Ni1···Ni3	4.827(5)	Ni2-OW3	2.058(6)
Ni1···Ni4	4.963(5)	Ni3−O31	2.092(4)
Ni1···Ni5	6.058(8)	Ni3−OW4	2.086(5)
Ni2···Ni3	3.367(3)	Ni3−OW5	2.067(5)
Ni2···Ni4	3.728(3)	Ni3−N22	2.048(5)
Ni2···Ni5	3.243(1)	Ni3−O23	2.076(5)
Ni3···Ni4	7.082(5)	Ni3−N31	2.050(5)
Ni3···Ni5	4.773(6)	Ni4−N2	2.084(7)
Ni4···Ni5	4.714(3)	Ni4−N3	2.078(6)
Ni1−O1	2.080(5)	Ni4−N11	2.106(5)
Ni1−O21	2.020(4)	Ni4−N12	2.057(5)
Ni1−OW1	2.119(5)	Ni4−OW6	2.120(5)
Ni1−OW2	2.049(5)	Ni4−OW7	2.099(5)
Ni1−N1	2.035(5)	Ni5−O11	2.060(4)
Ni1−N21	2.078(5)	Ni5−N13	2.095(5)
Ni2−O1	2.138(6)	Ni5−N32	2.070(5)
Ni2−O11	2.000(4)	Ni5−N33	2.064(5)
Ni2−O21	2.025(4)	Ni5−N41	2.099(5)
Ni2−O31	2.083(4)	Ni5−N42	2.025(5)
O1−Ni1−N21	166.5(2)	N2−Ni4−N11	170.3(2)
O21−Ni1−N1	166.6(2)	N3−Ni4−N12	174.0(2)
OW1−Ni1−OW2	177.1(2)	O11−Ni5−N33	159.5(2)
O1−Ni2−O31	166.0(2)	N13−Ni5−N42	158.9(2)
O11−Ni2−O21	175.8(2)	N32−Ni5−N41	166.5(2)
O41−Ni2−OW3	175.7(2)	Ni1−O1−Ni2	98.3(2)
O31−Ni3−N23	171.5(2)	Ni2−O11−Ni5	106.1(2)
OW4−Ni3−OW5	174.3(2)	Ni1−O21−Ni2	104.2(2)
N22−Ni3−N31	174.7(2)	Ni2−O31−Ni3	107.5(2)
OW6−Ni4−OW7	178.5(2)		

Magnetochemistry. Variable-temperature dc magnetic susceptibility studies were performed on powdered samples of compounds **1**−**3** in an applied magnetic field of 0.1 T (1.0 kG) and in the 5.0−300 K range.

The data for **1** and **2**·2H_2O are plotted as $\chi_M T$ vs T in Figure 8. $\chi_M T$ at 300 K is 21.07 and 20.84 cm^3 K mol^{-1} for **1** and **2**·2H_2O, respectively. The 300 K values are higher than the 16.94 and 14.52 cm^3 K mol^{-1} values (both for g = 2.2) expected for clusters of 14 and 12 noninteracting Ni^{II} atoms, respectively, indicating the presence of ferromagnetic exchange interactions. As the temperature is lowered, $\chi_M T$ for both complexes gradually decreases to a minimum at ∼90 (**1**) and ∼60 (**2**·2H_2O) K and then increases to 25.89 cm^3 K mol^{-1} at 6.5 K for **1** and 16.52 cm^3 K mol^{-1} at 6.5 K for **2**·2H_2O. The $\chi_M T$ values and the similar shape of the curves are consistent with both ferro- and antiferromagnetic interactions being present, promoted by the end-on N_3^- ions[35a,61] and the bridging OH$^-$/oximate groups,[14,15,25,26] respectively. Assuming typical[58a] g values for Ni^{II} of 2.2−2.3, the 6.5 K values for **1** and **2**·2H_2O suggest an S = 6 complex and

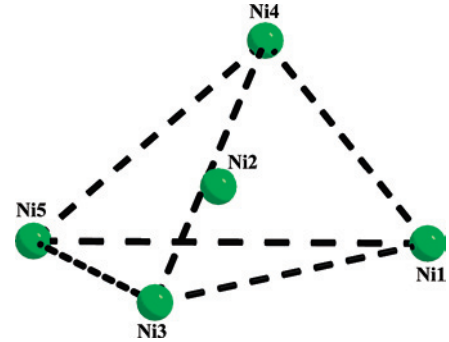

Figure 7. The Ni_5 skeleton of **3** emphasizing its very distorted tetrahedral metal topology.

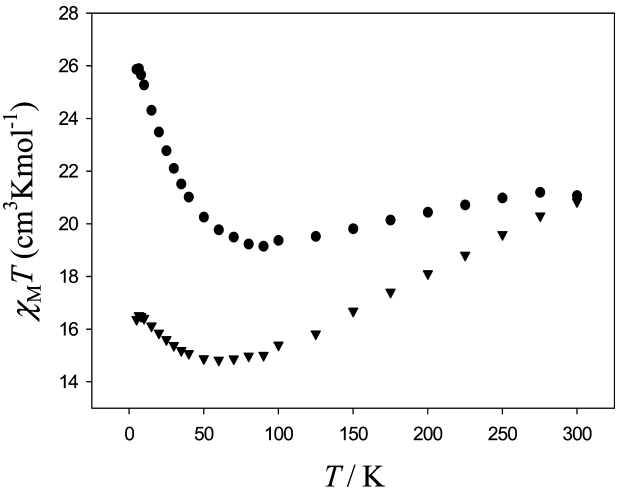

Figure 8. Plots of $\chi_M T$ vs. T for complexes **1** (●) and **2**·2H$_2$O (▼).

two essentially noninteracting $S = 3$ Ni$_6$ fragments, respectively; we expect the exchange interactions through the central Na$^+$ ions to be essentially zero and that **2**·2H$_2$O can thus be described magnetically as a dimer. Given the size and relatively low symmetry of the Ni$_{14}$ and Ni$_{12}$Na$_2$ cations and the resulting number of inequivalent exchange interactions, it is not possible to apply the Kambe method[62] to determine the individual pairwise Ni$_2$ coupling constants, and we concentrated instead on confirming the initial estimates of the ground state S values of the compounds and obtaining the D values.

Magnetization (M) vs dc field measurements were made on restrained samples of **1** and **2**·2H$_2$O in fields (H) up to 70 kG (7 T) and in the 1.8−10.0 K temperature range. Initial problems in fitting the data suggested complications from low-lying excited states, as expected for high-nuclearity complexes, and we obtained good fits by excluding the higher field data, above 4 T for **1** and above 1.0 T for **2**·2H$_2$O; similar problems have been reported for other Ni$_x$Na$_y$ clusters.[51] The resulting data and fits for **1** and **2**·2H$_2$O are shown in Figures 9 and 10, respectively; the data are plotted as reduced magnetization ($M/(N\mu_B)$) vs H/T, where N is Avogadro's number and μ_B is the Bohr magneton. The data were fit using the program MAGNET[63] to a model that assumes that only the ground state is populated at these temperatures and magnetic fields, includes the Zeeman interaction and axial zero-field splitting ($D\hat{S}_z^2$), and incorporates a full powder average. The corresponding spin Hamiltonian is given by eq 4, where $\hat{S}_z$ is the easy-axis spin operator and μ_0 is the vacuum permeability. The last term in eq 4 is the Zeeman energy associated with an applied magnetic field. The best fits (solid lines in Figures 9 and 10) gave $S = 6$, $g = 2.17(2)$, and $D = -0.12(3)$ cm^{-1} for **1** and $S = 3$, $g = 2.09(2)$, $D = -0.20(5)$ cm^{-1} for each of the Ni$_6$ subunits in **2**. For **1**, the fits for $S = 5$ and 7 were clearly unacceptable, giving $g > 2.5$ and $g < 1.9$, respectively.

$$\mathscr{H} = D\hat{S}_z^2 + g\mu_B\mu_0\hat{S}\cdot H \qquad (4)$$

As we have reported before on many occasions,[64] another way to avoid complications from the presence of a dc field and its effect on low-lying excited states is to use ac

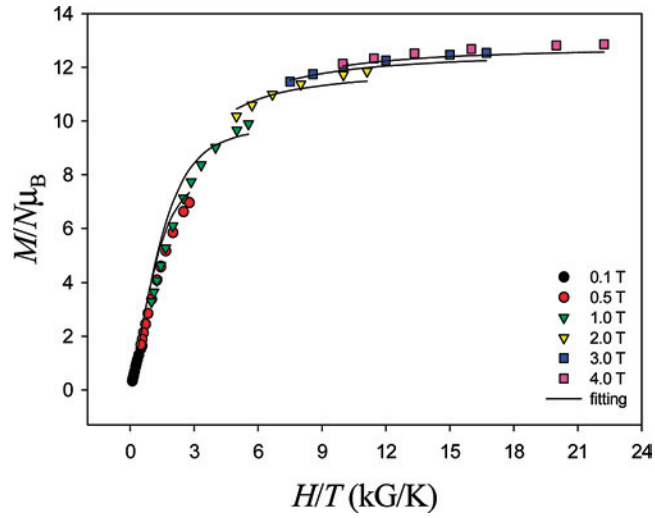

Figure 9. Plot of reduced magnetization ($M/(N\mu_B)$) vs H/T for complex **1** in the temperature range 1.8−10.0 K and at the indicated fields. Solid lines are the fits of the data; see the text for the fit parameters.

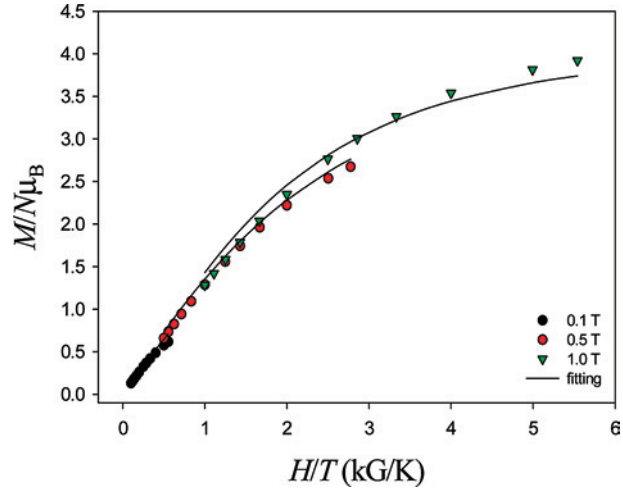

Figure 10. Plot of reduced magnetization ($M/(N\mu_B)$) vs H/T for complex **2**·2H$_2$O in the temperature range 1.8−10.0 K and at the indicated fields. Solid lines are the fits of the data; see the text for the fit parameters.

susceptibility studies to determine the ground state of a system. These were thus carried out on **1** and **2**·2H$_2$O in the 1.8−15 K range using a 3.5 G ac field oscillating at frequencies in the 50−1000 Hz range. Figure 11 shows the in-phase component χ'_M of the ac susceptibility, plotted as $\chi'_M T$ vs T: extrapolation of $\chi'_M T$ to 0 K, where only the ground state is populated and using data above ∼6 K (to avoid the low temperature drops due to weak intermolecular interactions and zero-field splitting) gave ∼23.5 and ∼7.8 cm^3 K mol^{-1} for **1** and each Ni$_6$ subunit of **2**, respectively, indicating an $S = 6$ ground state for **1** and an $S = 3$ ground state for each half of **2**, both with $g > 2$ as expected for Ni^{II}. Thus, the ac studies provide independent confirmation of the conclusions from the dc magnetization fits. Complexes

(61) Halcrow, M. A.; Sun, J.-S.; Huffman, J. C.; Christou, G. *Inorg. Chem.* **1995**, *34*, 4167.
(62) Kambe, J. K. *J. Phys. Soc. Jpn.* **1950**, *5*, 48.
(63) Davidson, E. R. *MAGNET*, Indiana University, Bloomington, IN, 1999.
(64) For example, see: Taguchi, Th.; Stamatatos, Th. C.; Abboud, K. A.; Jones, C. M.; Poole, K. M.; O'Brien, Th. A.; Christou, G. *Inorg. Chem.* **2008**, *47*, 4094.

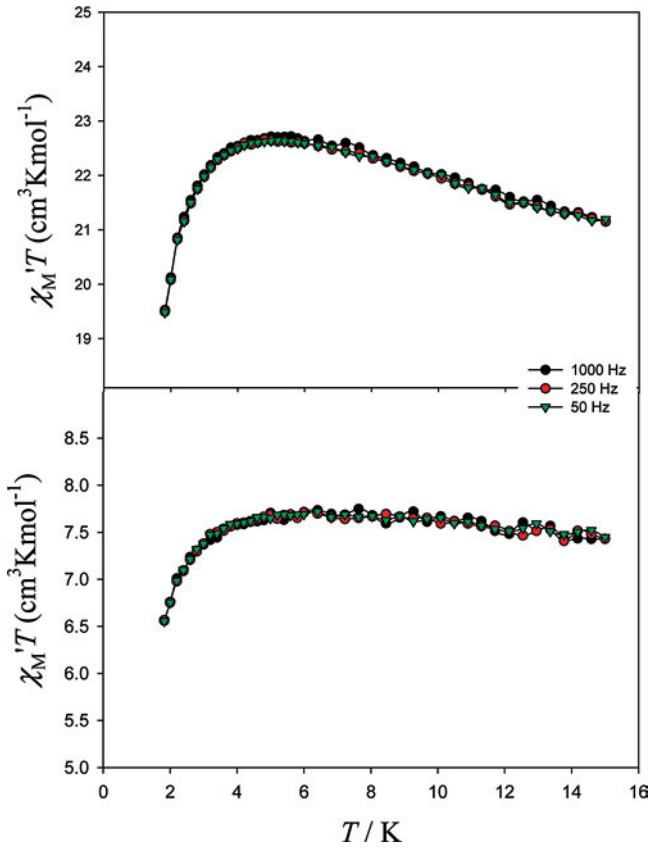

Figure 11. Plots of $\chi'_M T$ vs T at the indicated frequencies for cluster **1** (top) and **2** (bottom, per Ni_6 subunit).

1 and **2**·$2H_2O$ do not exhibit an out-of-phase (imaginary) ac magnetic susceptibility signal down to 1.8 K, the operating minimum of the SQUID magnetometer, suggesting they are not SMMs.

Owing to the size and complexity of the cores of **1** and **2**, it is not straightforward to unequivocally rationalize the observed ground states. An $S = 6$ ground state for a Ni^{II}_{14} complex such as **1** that has spin values in the $S = 0-14$ range is consistent with a combination of both ferro- and antiferromagnetic interactions. As a result, it is possible and even likely that the $S = 6$ ground state arises from competing exchange interactions and spin frustration effects, making it difficult to predict the precise ground-state spin alignments. One possibility can be offered with reference to Figure 2 and assuming that (i) all the interactions through the end-on N_3^- groups are ferromagnetic,[35a] (ii) the Ni2Ni2′Ni4Ni4′ central defective double-cubane subunit is ferromagnetically coupled (as found for discrete defective double-cubane Ni^{II} clusters possessing exclusively monatomic O bridges, albeit with slightly smaller Ni−O−Ni angles, which have an $S =$ 4 ground state,[65] and (iii) the Ni2···Ni(1,3), Ni2···Ni(6,7) and their symmetry equivalent interactions are antiferromagnetic due[56] to the large Ni−O−Ni angles involved (110.3°−112.5°). If these assumptions are valid, then the predicted ground state is $S = 10 - 4 = 6$, as found experimentally. Of course, this is only one reasonable possibility, among others. Note also that the same argument would suggest an $S = 4$ spin for each half of **2**, which is close to but nevertheless higher than the experimental $S = 3$, emphasizing that the true spin alignment situation in these complexes is indeed more complicated than the simple spin-up/spin-down picture offered for **1**.

(65) (a) King, P.; Clérac, R.; Wernsdorfer, W.; Anson, C. E.; Powell, A. K. *Dalton Trans.* **2004**, 2670. (b) Clemente-Juan, J. M.; Coronado, E.; Galán-Mascarós, J. R.; Gómez-García, C. J. *Inorg. Chem.* **1999**, *38*, 55.

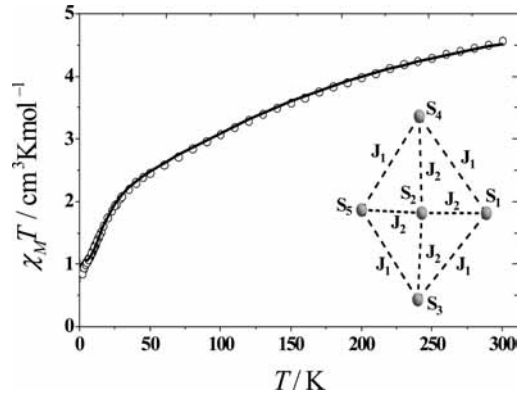

Figure 12. Plot of $\chi_M T$ vs T for complex **3**·$2H_2O$. The solid line is the fit of the data; see the text for the fit parameters. The inset is the 2-J exchange coupling model used.

The data for **3**·$2H_2O$ are plotted as $\chi_M T$ vs T in Figure 12. $\chi_M T$ at 300 K is 4.57 cm^3 K mol^{-1}, lower than the spin-only ($g = 2.2$) value of 6.05 cm^3 K mol^{-1} expected for a cluster of five noninteracting Ni^{II} atoms. $\chi_M T$ decreases steadily with decreasing temperature to 2.32 cm^3 K mol^{-1} at 40 K, before decreasing rapidly below this temperature to 1.06 cm^3 K mol^{-1} at 5.0 K. This behavior indicates the presence of dominant antiferromagnetic exchange interactions and a low, but possibly nonzero, ground-state S value. The $\chi_M T$ value at 5.0 K is consistent with an $S = 1$ ground state, for which the spin-only ($g = 2.2$) value is 1.21 cm^3 K mol^{-1}. Magnetization data collected at 2.0 K show a Brillouin-shaped curve with a value close to two electrons, supporting an $S = 1$ ground state.

Inspection of the structure of **3** (Figures 5 and 6) reveals that by symmetry there are eight different nearest-neighbor Ni···Ni exchange interactions, which can be collected into five groups on the basis of their superexchange pathways: J_A (the Ni1···Ni2 interaction through two bridging oximate O atoms), J_B (the outer Ni1···Ni3, Ni3···Ni5, Ni5···Ni4, and Ni4···Ni1 interactions through one diatomic oximate group from an $\eta^1{:}\eta^1{:}\eta^2{:}\ \eta^1{:}\mu_3$ ppko$^-$ ligand, with very similar Ni···Ni distances, Ni−O−N and Ni−N−O bond angles, and Ni−N−O−Ni torsion angles); J_C (the Ni2···Ni3 interaction through one bridging oximate oxygen and one μ_3 diatomic oximate group); J_D (the Ni2···Ni4, interaction through two μ_3 diatomic oximate groups); and J_E (the Ni2···Ni5 interaction through one bridging oximate oxygen, one μ diatomic oximate group, and one μ_3 diatomic oximate group). The spin Hamiltonian for this model is given by eq 5.

$$H = -J_A(\hat{S}_1 \cdot \hat{S}_2) - J_B(\hat{S}_1 \cdot \hat{S}_3 + \hat{S}_3 \cdot \hat{S}_5 + \hat{S}_5 \cdot \hat{S}_4 + \hat{S}_4 \cdot \hat{S}_1) - J_C(\hat{S}_2 \cdot \hat{S}_3) - J_D(\hat{S}_2 \cdot \hat{S}_4) - J_E(\hat{S}_2 \cdot \hat{S}_5) \quad (5)$$

A preliminary fit of the experimental data with the program CLUMAG,[66] applying the above Hamiltonian, gave as best

fit parameters $J_B = -20.3$ cm^{-1}, $J_A = J_E = -41.5$ cm^{-1}, $J_C = J_D = -43.9$ cm^{-1}, and $g = 2.20$. This was somewhat unexpected because we had anticipated that the interactions between Ni2 and Ni(1,3,4,5), that is, J_A, J_C, J_D, and J_E, would all be different due to the different types of bridges involved. On the basis of this preliminary result, our desire to avoid overparameterization, and the very small changes in the shape of the $\chi_M T$ vs T plot induced by small variation of J_A, J_C, J_D, and J_E, we decided to fit the data using the 2-J coupling scheme shown as the inset of Figure 12, that is, with $J_B = J_1$ and $J_A = J_C = J_D = J_E = J_2$. The corresponding spin Hamiltonian is given in eq 6, and the best-fit parameters with this model were $J_1 = -21.8$ cm^{-1}, $J_2 = -45.9$ cm^{-1}, and $g = 2.24$.

$$H = -J_1(\hat{S}_1 \cdot \hat{S}_3 + \hat{S}_3 \cdot \hat{S}_5 + \hat{S}_5 \cdot \hat{S}_4 + \hat{S}_4 \cdot \hat{S}_1) - J_2(\hat{S}_1 \cdot \hat{S}_2 + \hat{S}_2 \cdot \hat{S}_3 + \hat{S}_2 \cdot \hat{S}_4 + \hat{S}_2 \cdot \hat{S}_5) \quad (6)$$

The obtained J values are in satisfactory agreement with the antiferromagnetic exchange coupling constants found for other pyridyl oximate-bridged Ni^{II} complexes.[13,14,25,26,58a] The bridging diatomic =N−O$^-$ group is known to be very efficient in mediating a medium-to-strong antiferromagnetic interaction, which is provided by an orbital exchange pathway of σ symmetry.[25] In addition, the antiferromagnetic J_2 coupling is further justified by the relatively large Ni−O(1,11,21,31)−Ni angles, which are in the 98.3(2)°−107.5(2)° range.[26b,27,59b]

For a system of five $S = 1$ centers that interact according to the 2-J model of eq 6, all ground state S values between 0 and 3 are possible depending on the J_2/J_1 ratio (Figure 13). In other words, since all J values are antiferromagnetic, there will be competing interactions within the many Ni_3 triangular subunits of **3** and resulting spin frustration effects, with the individual spin alignments at each metal thus being determined by the relative magnitudes of the competing interactions. When the dominant antiferromagnetic interaction is J_1 ($J_2/J_1 < 0.5$), the local spin of the outer Ni_4 subunit is 0 and the spin of the central atom Ni2 determines a ground-state of $S = 1$. In the format $|S,S^*,S'\rangle$, where S^* is the spin resultant for the outer Ni1, Ni3, Ni4, and Ni5 atoms and S' is the central spin, the ground state is $|1,0,1\rangle$. At the other limit, when the dominant antiferromagnetic interaction is J_2 ($J_2/J_1 > 4.0$), the interaction between the central and outer metal atoms dominates and the ground state has $S = 3$, the $|3,4,1\rangle$ state. Between these two limits, in the special cases of $J_2/J_1 = 0.5$, 2.0, 3.0, and 4.0, a degeneracy appears in the ground-state between states with total spins 1 and 0, 0 and 1, 1 and 2, and 2 and 3, respectively. In the case of cluster **3**, the experimental J_2/J_1 value is 2.1, consistent with the region for an $S = 1$ ground state in Figure 13.

Conclusions and Perspectives

The present work extends the body of results that emphasize the ability of the monoanionic ligands pao$^-$ and ppko$^-$ to form interesting structural types in 3d metal chemistry. The use of both pao$^-$ and N_3^- in reactions with Ni^{II} sources has led to products **1** and **2**, the highest nuclearity metal/oxime and Ni^{II}/N_3^- clusters to date, showing that 2-pyridyl oximes can indeed support high nuclearity chemistry when combined with appropriate ancillary inorganic ligands. The obtained Ni_{14} and $Ni_{12}Na_2$ products are novel in multiple ways, as described, but they also provide a rare example of a complicated structural type where paramagnetic ions have been replaced with diamagnetic ones with negligible impact on the structure. The work described above demonstrates the synthetic novelty that arises when N_3^- is used in conjunction with 2-pyridyl oxime ligands, the beauty of the resulting molecules/ions, and the interesting magnetic properties these compounds possess. The reaction of Ni^{II} with ppko$^-$ in the presence of NO_3^- and in the absence of N_3^- ions has given the Ni$^{II}_5$ cluster **3** with a novel core. The different (compared with pao$^-$) coordination characteristics of ppko$^-$ and the absence of N_3^- ligands fostered formation of a product completely different from that of the azide clusters **1** and **2**. It is also interesting that all the NO_3^- groups in **3** behave as counterions giving an unusual pentacationic cluster. The magnetic properties of **3** have been interpreted using two exchange interactions in a simplified model. The study also revealed that this complex possesses an $S = 1$ ground state because of the particular ratio of its J values.

We have no reason to believe that this research area is exhausted of new results. Indeed, ongoing studies are producing additional and interesting products, and our belief is that we have scratched only the surface of metal cluster chemistry based on pyridyl oximate ligands. As far as future perspectives are concerned, analogues of **1** and **2** with methyl (mpkoH; Scheme 1) and phenyl [(ph)pkoH; Scheme 1] 2-pyridyl ketone oxime are not known to date, and it is currently not evident whether the preparation and stability of such Ni$^{II}_{14}$ and Ni$^{II}_{12}$Na$^{I}_2$ clusters are dependent on the particular nature of the R substituent on the oxime carbon. Ni^{II}/ppko$^-$/N_3^- chemistry is also completely unexplored, and work currently in progress is unearthing interesting new clusters. Since the μ_3-OH$^-$ groups in **1** and **2** most probably propagate antiferromagnetic exchange interactions (e.g., the Ni2···Ni1 and Ni2···Ni7 interactions in **1**), we are also pursuing the substitution of the OH$^-$ bridges by end-on N_3^-

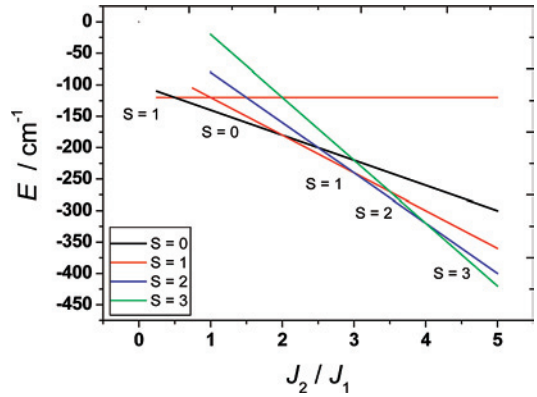

Figure 13. Energy-level diagram showing the ground-state variation with respect to the J_2/J_1 ratio for a system of five Ni^{II} atoms that interact according to the model shown in the inset of Figure 12. The energy values have been calculated for an arbitrary J_1 value of -20 cm^{-1}.

(66) Gatteschi, D.; Pardi, L. *Gazz. Chim. Ital.* **1993**, *123*, 231.

groups in order to introduce more ferromagnetic components in the superexchange scheme.

Acknowledgment. A.E. thanks the Ministerio de Educación y Ciencia (MEC) for financial support (Grant CTQ2006-01759). S.P.P acknowledges funding from the Operational and Vocational Training II (EPEAEK II) and particularly the program PYTHAGORAS I (Grant b.365.037). G.C. thanks the National Science Foundation (Grant CHE-0414555) for support of this work.

Supporting Information Available: Crystallographic data in CIF format for the three compounds, figures showing the Ni^{II}_4 and Ni^{II}_5 subunits of the core of complex **1** (Figure S1), and a detailed view of the core of complex **2** (Figure S2). This material is available free of charge via the Internet at http://pubs.acs.org.

IC801555E